SACLANTCEN REPORT
serial no: SR-291

SACLANT UNDERSEA RESEARCH CENTRE REPORT

DEPLOYABLE UNDERWATER SURVEILLANCE SYSTEMS. LOCALIZATION AND FUSION OF MULTISTATIC CONTACTS. EVALUATION OF FEASIBILITY USING EXPERIMENTAL DATA

L. Mozzone, S. Bongi

December 1998

Report no. changed (Mar 2006): SR-291-UU

This document is approved for public release.
Distribution is unlimited

SACLANT Undersea Research Centre
Viale San Bartolomeo 400
19138 San Bartolomeo (SP), Italy

tel: +39-0187-540.111
fax: +39-0187-524.600

e-mail: library@saclantc.nato.int

NORTH ATLANTIC TREATY ORGANIZATION

Deployable Underwater Surveillance Systems. Localization and fusion of multistatic contacts. Evaluation of feasibility using experimental data.

L. Mozzone, S. Bongi

The content of this document pertains to work performed under Project 021-1 of the SACLANTCEN Programme of Work. The document has been approved for release by The Director, SACLANTCEN.

Jan L. Spoelstra
Director

intentionally blank page

Deployable Underwater Surveillance Systems. Localization and fusion of multistatic contacts. Evaluation of feasibility using experimental data.

L. Mozzone, S. Bongi

Executive Summary: Prototype active sonar deployable underwater surveillance systems (DUSS) are being developed at SACLANT Undersea Research Center to respond to NATO operational requirements. The concept is based on a distributed network of small autonomous nodes (transmitters / receivers) integrated into a multistatic system. The limited coverage of each node is extended by deploying multiple elements, thus building a modular network tailored to the operational needs of each mission. The integration of diverse receivers into a single sonar system requires accurate and consistent measurements of target positions.

This study assesses the target localization performance of individual DUSS sonar nodes. Experimental data collected with the test system during the campaign "DUSS'97" are discussed. 450 pings are analyzed on 3 receivers. An echo repeater target with differential GPS positioning was towed in 3 types of trajectory at 2 frequencies. In spite of the limited resources of the small DUSS nodes tested, overall positioning error medians are as low as 118 m in the range of target trajectories of the experiments (maximum distance of 23 km). Monostatic and multistatic nodes perform similarly. Pulse frequency and target trajectory type do not noticeably affect the results. The results are interpreted and discussed with the aid of simple theoretical models, which estimate the sensitivity of overall performance to the most relevant characteristics and parameters of the system. Reference objectives and specifications are therefore provided to prototype design activities. The maximum specified bias and standard deviation values are: 20 m in the knowledge of assets deployment positions; 5 m in the in-buoy DGPS; 0.1° in the compass and 4‰ in the length of acoustic propagation paths. The experience acquired in all issues related to contact localization with DUSS is also reported, from mechanical structure of the deployable buoy to sensor precision, array design and computing issues.

Recommended beamwidths range between 7° and 4°; values which are compatible with the performance provided in the experiments by other critical factors such as the quality of compasses, the accuracy and rigidity of mechanical assembly, the measurability of sonar deployment positions.

The feasibility of effective and consistent fusion of the contacts obtained from multiple receivers is also discussed. The median of spreading of contacts on the three receivers is limited to 70 m. The integration of DUSS receivers into a network of cooperating sonar nodes requires contact association windows of an estimated maximum of 100 bearing - range cells. The possibility of improving measurement accuracy by merging contacts is shown. Using a very simple method, which averages out the contact localization data from the three receivers, a 22% reduction of the median of error is obtained.

The experience and results reported here are directly applicable to the design of prototypes. Tests with real data fusion algorithms would be beneficial in finalizing beamwidth requirements. The localization of deployed assets is a critical factor. More attention should be given to the area of data fusion and processing gain.

intentionally blank page

Deployable Underwater Surveillance Systems. Localization and fusion of multistatic contacts. Evaluation of feasibility using experimental data.

L. Mozzone, S. Bongi

Abstract: Active sonar deployable underwater surveillance systems (DUSS) are based on a distributed network of small multistatic transmitter / receiver nodes. This study analyzes the contact localization capabilities of DUSS with experimental data and simple modelling. Localization error medians of 118 m were measured analyzing 450 pings on 3 receivers in 2 frequencies and 3 target trajectories. This error produces a scattering of the contacts of the three receivers around their "barycentre", which is assumed by the multistatic system as the best estimation of the target position. Such scattering was found to be limited to an overall median value of 110 m. The integration of the distributed sonar nodes into a single, extended surveillance system is therefore possible with contact association windows of that size, corresponding to about 100 bearing - range cells. The resulting improvement of contact localization errors was estimated at around 22%. Efficient data fusion methods can therefore be investigated with good expectations. The experimental results do not depend on frequency, target range and trajectory, receiver monostatic / multistatic deployment geometry. Performance objectives and system specifications are also derived for prototype design. The precision of compasses and asset deployment positioning are the most critical parameters.

Keywords: Active, Deployable, Multistatic, Sonar, Localization, Bearing, GPS, Experiment, Data fusion.

Acknowledgments

This work was made possible by the coordinated efforts and the enthusiasm of the technical support and ships' personnel of SACLANT Centre. In fact it deeply relied on all the fields of expertise being cultivated at the Centre for the collection and processing of a large set of experimental data. A special thank to D. Hughes and J. Ziegenbein for their support and constructive criticism.

Contents

1

Introduction

Deployable underwater surveillance systems (DUSS) are being developed at SACLANT Undersea Research Centre. DUSS consists of a distributed network of **small**, low cost and/or expendable **active** sonar systems optimized for **multistatic** operation in **shallow** and coastal waters against **small targets**, in the presence of heavy shipping **traffic** and strong **reverberation**. The objective of this project is the investigation and assessment of performance potentials of the DUSS concept by means of experimental campaigns conducted with a test system, and the final formulation and trial of an optimized concept demonstrator. This report is the fourth of a series of documents which describe the characteristics of the experimental system and the results of tests at sea [1, 2, 3], quantifying the detection performance of DUSS. This study analyzes the contact localization potential of deployable underwater surveillance systems in shallow water and reports the measurements collected in controlled conditions, with a calibrated Echo Repeater, during the experiment "DUSS '97" conducted at sea on 29 June - 4 July, 1997, south of the Island of Elba, (Italy).

This study has the following objectives:

- To quantify the contact localization performance of the test system in the experiments. Two frequencies and three different target trajectories were tested with two multistatic and one monostatic receivers.

- The analysis of which system characteristics and parameters most determine contact localization errors and the estimation of overall system performance sensitivity to those parameters. This is accomplished with simple models that simulate the contact localization process and estimate the effects of the most relevant sources of error on the system by means of simple Monte Carlo simulations.

- The formulation of tradeoffs and specifications for the design of an optimal prototype. The experience acquired in all issues related to contact localization with DUSS is also reported, from mechanical structure of the deployable buoy to sensor precision, array design and computing issues.

- The evaluation of the scattering of contacts localized by different receivers. The feasibility of multistatic data fusion is experimentally assessed. Indications about the width of contact merging windows (on which data fusion overheads depend) are also obtained.

- The demonstration of overall localization precision improvement deriving from multiple receivers.

The following sections describe the DUSS sonar concept (Sect. 2), the test system (Sect. 3), the experiment "DUSS '97" (Sect. 4) [1, 2, 3]. The sources of localization errors are discussed and simulation results are produced (Sect. 5) for subsequent comparison with experimental results (Sect. 6). Conclusions are summarized in Sect. 7, recommendations for further work are given in Sect. 8.

2

The concept of deployable underwater surveillance systems (DUSS)

The main requirement of this project derives from the need to achieve a higher degree of control upon water volumes where the sonar problem is more complex. Severe echo attenuation and distortion, sound interaction with boundaries, shipping noise and reduced target response lead the sonar designer towards a modular, distributed concept based on a network of small sonar nodes. The proposed system is thus shifted towards a more favorable position in the ideal curve of performance *versus* complexity, where reduced but more robust and reliable surveillance ranges (volumes) can be obtained with a much smaller effort. The limited individual coverage is enhanced by the usage of multiple sonar nodes (either receivers or transmitters) deployed at different locations and depths. The latest advances in communication, signal processing and electronics are necessary to create and integrate such an autonomous distributed system. This report also demonstrates the advantages of DUSS in terms of receiver covertness, modularity, interoperability, reduced impact and risk, extended detection opportunities, contact localization accuracy (Fig. 1).

3 The test system

Experiments were conducted with the test system described in Annex A, The receivers include 25 hydrophones in a planar, star shaped structure with 5 arms optimized for the two working frequency bands of 1.9 and 3.5 kHz (Fig. 2). They are battery powered, moored to the sea bed, and transmit base banded acoustic and compass data *via* radio to the laboratory on *Alliance*. Table 1 shows beam pattern characteristics.

Table 1 *Beam widths at -3 dB in degrees, DI and horizontal Array Gain (AG_H) in dB:*

Frequency	Horizontal	Vertical	DI	AG_H
1900 Hz	13.2°	54.6°	13.3 dB	12.5 dB
3500 Hz	7.1°	40.7°	12.9 dB	11.3 dB

The transmitters are directive on the vertical plane for minimum interactions with sea boundaries. They hang alongside the moored ship with Receiver 1. The real time data acquisition, processing and display system is described in [1], Annex D. The Echo Repeater, towed by the NATO R/V *Manning*, digitally stores and transmits back impinging pulses with a known, high target strength. Measured radiation patterns are shown in [1]. Trajectories and frequency bands were planned to have nominal, aspect independent target strength in all cases. Depth of tow is electronically logged. A very important element of the multistatic test system is the precise localization of all assets (deployed transmitters, receivers, trajectories of target, drifting of the moored ship) for post-test analysis. It is accomplished *via* log-files of differential GPS and radar. The latter also provides the means to monitor traffic conditions.

4

The experiment DUSS '97

The experiment was conducted from 29 June to 4 July 1997, south of the Island of Elba (Italy). The test area (Fig. 3) is highly representative of DUSS requirements, namely intense shipping traffic, unfavourable sound velocity profile, shallow sloping bottom with continuous reverberation, bottom features and echoes from islands.

The echo repeater simulated a target by digitally storing and transmitting back the impinging pulses received from the acoustic transmitter. It was towed along selected trajectories comprising the most significant aspect and distance configurations of a multistatic surveillance system. Five runs and 450 pings are analyzed in this study. Three receivers were deployed in a constant depth line (Fig. 3) at 2 n.mi intervals. Receivers 2 and 3 were moored on the sloping continental shelf, over a bottom 160 m deep. The transmitters were suspended overboard from *Alliance* on station at a fixed position, with the monostatic Receiver 1. LFM pulses of 1 s duration were used.

Acoustic data were stored, processed in real time and displayed on board *Alliance*, for quality monitoring and real time detection. Geographical information is of paramount importance in multistatic sonar operation. Positions of sonar assets and the ship from differential GPS and radar were stored and monitored. The multistatic geometry of experiments was reconstructed in real time on a personal computer and during the analysis, including data from the submarine logs. Such reconstructed data were cross-checked with acoustic contact localization. Radar tracks of shipping traffic were stored and monitored for protecting the deployed assets, assessing the effects of interfering noise and further validating the acoustic contacts. Sound velocity profiles, sea state, currents and weather conditions were regularly sampled and recorded in log books and digital files. Bathymetry measurements were collected with the ship's echo sounder during sound velocity profile surveys. Accurate charts were recorded of the areas where the experiment took place, for safe and optimal deployment and for range dependent propagation modelling. Acoustic source and target depths during tow were recorded in digital files.

Careful interpolation of Echo Repeater DGPS position and compensation of transmission delay were necessary in the analysis. The beamformer continuously re-computes beams directions to compensate for buoy rotation.

4.1 Environmental conditions

Environmental data were regularly collected and recorded during experiments by means of the ship's meteorological system. Written log book summaries were extracted. During the experiment the average sea state was 3-4, with winds around 8-12 kn for most of the time. Sunny days alternated with cloudy days. As a consequence of the weather, the SVP maintained a surface mixed layer, about 20 m deep, followed by the strong gradient typical of the season (18 m/s variation in 20 m of depth, Fig. 4). Velocity increase with depth in the isothermal column below 70 m was very moderate or absent, which prevented the formation of a deep propagation channel. Propagation was thus dominated by the strongly absorbing bottom, determining high propagation losses. Average recorded currents were about 0.3 kn. Shipping traffic was very intense throughout the experiment.

4.2 Performed Runs

The experiment is divided into "runs", each of which is characterized by a particular trajectory of the target and pulse type. Target trajectory types "A", "C", "D" are shown in Fig. 3. Run identification codes include day and run number (e.g. 0103 means July 1st, 3rd run).

Speed of target: 5 kn.

Pulse: LFM, 1 second duration, 200 Hz bandwidth. A delayed CW "tag" of 180 dB, 0.25 s.

Pulse repetition rate: 60 s.

Source levels: 205.5 dB at 3500 Hz, with a variability of ± 2.5 dB with bearing, and 204 dB at 1900 Hz, omnidirectional.

Source vertical directivity: vertical dipole at 900 Hz, 10 elements vertical string at 1900 Hz, 5 elements at 3500 Hz.

Depth of receivers: 110 m.

Target strength: 30 dB simulated by the echo repeater.

Table 2 *Summary of runs.*

RUN	Frequency kHz	Pulse duration s	Duration min	Source depth m	Target depth m	Target trajectory
0103	3.5	1 s	90	110	90	C
0201	1.9	1 s	120	80	90	C
0203	3.5	1 s	120	110	90	A
0104	3.5	1 s	60	110	90	D
0200	1.9	1 s	60	80	90	D

5

Modelling and analysis of localization errors

Many possible sources of error may affect localization precision of a multistatic system. This section summarizes them and analyzes their effects on the whole system by means of simple models. The processes of bearing estimation and geometry reconstruction of the experiment are modelled, and the sensitivity of the system to the perturbation of individual parameters is observed with Monte Carlo simulations. The relative importance of the various independent effects can therefore be assessed and a better understanding of experimental results (Sect. 6) can be achieved. Design criteria are also produced for the specification of a prototype. The number of simulation runs was gradually increased with repeated trials until, around 10000, stable results were obtained, with differences of less than 5% between independent simulations. Localization data are expressed in terms of latitude - longitude coordinates and the corresponding errors in terms of distances (km). This criterion was preferred to the more classical bearing - range (or delay) coordinates because it better fits the multistatic structure of DUSS, where the same position corresponds to different bearings and delays for the different receivers.

5.1 Compass errors

Compass bias due to receiver array assembly may produce positioning errors. Such tolerance cannot be eliminated due to the intrinsic precision limitations of mechanical frames of deployable systems. However it can be partially corrected after deployment by using a reference object with a known position (e.g. the transmitter).

A trivial example of a bias of 1° is shown in Fig. 5.

The compass built in the receivers has a 10 bits quantization capability, which corresponds to steps $q = 0.351°$. The corresponding error can be represented as a uniformly distributed random variable with zero mean and standard deviation $\sigma_c = 0.1°$, obtained with the following formula [4].

$$\sigma_c^2 = \frac{1}{q}\int_{-q/2}^{+q/2} q^2 dq = q^2 / 12$$

The resulting contact localization error has zero mean and a standard deviation shown in Fig. 6a. The example is referred to the actual configuration of the system during the experiment, the transmitter and receiver number 3 are shown as circles.

Note that in both cases (bias and random bearing error) the resulting localization errors increase with the distance from the receiver.

5.2 Timing errors

Transmission timing and acquisition synchronization across all receivers must be accurate. For the sake of completeness, an example is shown in Fig. 7 of errors deriving from a mismatch of 17 ms (10 acquisition samples). Note that errors do not diverge with increasing distance from receivers. The precision achieved during experiments was superior to the simple constant error of 12.8 in a monostatic case.

Note that the same time error can be interpreted as a mismatch between expected and actual pulse travel time. This can be due to errors in the measurement of the speed of sound or to insufficient knowledge of the structure of the propagation paths on the vertical plane, which may differ from the simple assumption of straight lines. The example considered here, of a 17 ms error, corresponds to a range error of 1‰ (one part in a thousand) at 13 km, with a resulting error of 13 - 18 m (Fig. 7). An error of 4‰ e.g. in sound speed at 20 km corresponds to errors of 100 - 140 m.

5.3 Sonar positioning errors

Errors in the knowledge of the position of sonar nodes (transmitter or receiver array) produce errors in the localization of contacts. They may derive from:

- Global Positioning System approximations.
- Random displacement between the deploying ship (*Alliance*) and the final asset position.
- Drifting of the mooring.
- Tilting of mooring cable due to currents.

Even if a differential GPS system were installed on sonar nodes, unpredictable displacement would exist between the floating buoy with the GPS receiver and the submerged acoustic array. The need to keep the float on the surface increases the scale of the error.

Such errors are modelled here as either deterministic off-set (drifting) or two-dimensional random processes with two independent Gaussian distributions in latitude and longitude. It is difficult to estimate the extent of these errors, even after four experimental campaigns at sea. Values between 5 m for very careful experiments and 20 m for operational systems deployed in adverse conditions can be assumed. A variance of 5 m

can be assumed for differential GPS. Specifications report values between 1 m and 3 m for optimal satellite conditions and short distances from the differential reference station [5].

The results of Monte Carlo simulations are shown in Fig. 8 for a Root Mean Square (RMS) error of 5 m and 20 m in receiver position. Figure 9 shows the effects of a deterministic bias of 5 m and 20 m of the receiver.

It is important to note that the system is not very sensitive to these errors, and does not amplify them (with the exception of very close ranges).

5.4 Separation of multistatic deployment

The distance between source and multistatic receiver does not noticeably affect the resulting localization performance. Test cases were computed with an 8 n.mi source-receiver distance, time delay, bearing (Fig. 10) and receiver positioning errors. The resulting localization error does not differ significantly from the error obtained with a source - receiver separation of 4 n.mi (the difference is less than 5%).

5.5 Doppler - range ambiguity

The Doppler-range ambiguity of the LFM pulses needs to be corrected, taking into account the pulse characteristics and the different Doppler shift of each echo on each receiver. In an operational context, such shift can be measured (if double CW-LFM pulses are being used) or estimated from the tracking of contacts. With a 5 kn target speed, Doppler - range ambiguity produces a maximum error of 35 m on "A" type runs, [6]. It therefore represents a negligible share of the resulting errors, (as shown from the results in Sect. 6, with much larger errors). However, this systematic error component was removed from the experimental data by correcting all measured echo time delays on all receivers with the target trajectory characteristics (known from DGPS data).

5.6 Signal to Noise Ratio

Signal to noise ratio (SNR) is an important parameter determining bearing estimation accuracy. Noise interacts with the beampattern and introduces a random perturbation in the apparent direction of the maximum of SNR. The classical Cramer Rao bound formula estimates the lower bound for the standard deviation of bearing estimation [7]:

$$\sigma_\theta = \lambda / (L \sqrt{SNR_{out}})$$

where SNR_{out} is computed at the sonar output and L is the RMS array aperture length. For a simple linear array of length "l": $L = \pi l / \sqrt{3}$. An array with l = 3 m provides the same -

3 dB beamwidth of the receivers used here (13° at 1.9 kHz and 7° at 3.5 kHz). The resulting σ_θ is plotted in Fig. 10 as a function of SNR. Due to the high target strength provided by the echo repeater, most of the contacts analyzed here had SNRs above 25 dB, which correspond to $\sigma_\theta < 0.25°$ (at 3.5 kHz) and $\sigma_\theta < 0.5°$ (at 1.9 kHz). The influence of SNR on the experimental results is therefore limited (Fig. 6b). The effects of system characteristics other than detection SNR, are dominant in most of the experimental runs. Lower detection SNR values, more commonly encountered in sonar surveillance operations, e.g. 15 dB, would provide the result shown in Fig. 6c. A maximum σ_{C_Rao} of 250 m (defined here as the standard deviation of localization errors in metres due to SNR) is found at maximum ranges of 20 km. This information will be used as a reference for comparisons with the experimental results of the next section.

5.7 Summary

This section has analyzed the effects of the most important sources of approximation in the contact localization capability of a multistatic system. Simple deterministic and stochastic models were computed, using the characteristics of the existing test system as a reference. The results will be used in the next sections as a key to interpret the analysis of experimental data. Compass bias is the most critical factor. Precise mounting of the sensor frame of and coupling with the compass are essential to avoid performance degradation. Calibration after array deployment by means of known source location is also possible. Quantization and noise on compass measurements require particular attention. The timing of acoustic transmission and reception and the existing Differential GPS positioning hardware, on the contrary, provide satisfactory precision. It is recommended that the mooring location of assets with DGPS be monitored in real time. Random displacements between the DGPS floating buoy and the submerged acoustic receiver can be an important source of errors, requiring accurate engineering of the moorings. Additional sensors in the mooring cable to compensate for this critical error may also be considered. Finally, the weak SNR of barely detected real targets may dominate localization accuracy in critical conditions. With a detection SNR of 15 dB and 7° beams, a localization error with $\sigma_{C\_Rao} = 250$ m is found within 20 km of the receiver. Discussions on this subject will be resumed in Sect. 6.7, where specifications for beamwidths are expressed. That the experimental data had a high SNR allowed evaluation of the effects of non SNR related errors.

6
Data Analysis

This section analyses the data collected by the three receivers with the echo repeater target during experimental runs. Target acoustic localization is compared with DGPS information, which is very precise, with a standard deviation of 5 m [5]. Conclusions about the precision obtained are drawn. Also, potentials for inter - receiver data fusion emerge from this analysis.

6.1 Compass data

The analysis of compass time series provides useful information about the behaviour of the moored receivers and the localization precision that can be achieved in a real system. The hydrophone structure, symmetrical and star-shaped, rotates very slowly due to sea currents (Fig. 11). A faster fluctuation is superimposed on the measurement (Fig. 12): its rapid variations (its spectrum) suggest an interpretation in terms of uncorrelated, white noise added to the actual values. This noise is probably of electrical origin.

The standard deviation of noise is $\sigma_n = 0.3°$ larger than expected from quantization alone. It can be reduced by smoothing the compass series (i.e. by low-pass filtering) with a running integration window. The length of the window determines the noise reduction; in the hypothesis of white input noise (uncorrelated samples, as supported by the analysis of the autocorrelation of compass data) the reduction of σ_n is $\sqrt{N}$ (i.e. 10log(N) in dB for σ^2). In the typical cases shown above, an average over the whole ping file (40 s, 80 samples) can be used, with a potential reduction of 1:8.9 (19 dB), and $\sigma_n < \sigma_c$, the standard deviation due to quantization error only. A limit to such improvement is the speed of rotation of the array. Deployed arrays rotate slowly, due to currents. The available data show a maximum speed of 1°/min. Beamformer parameters have to be re-computed several times (about ten) during each ping interval (1 min). In some exceptional cases, receiver 1 rotated very rapidly (Fig. 14). It was hanging from the moored ship and fast rotations were probably induced by pitching. In these cases, the integration window can not be longer than 5 samples, but an acceptable degree of noise reduction can be expected ($\sigma_n = 0.3 / \sqrt{5} = 0.13° \approx \sigma_c$). The rotation produced an unpredictable scattering of bearing measurements around the real values in a couple of runs on Receiver 1, see Paragraph 6.3 below, due to the slow dynamic response of the compass, which could not trace properly the movements of the array. A fin in the hydrophone structure may eliminate fast rotation and vibration and the related problems of dynamic response of the compass to rapid variations and bearing data processing. A residual rotation induced by currents may be expected, with a speed of 1°/min.

Compass bias values up to 9° were found in the experimental system, due to the compass mounting and the flexible structure of hydrophones. Also magnetic variation contributes to a limited extent to bias errors. It was possible to correct bias with a satisfactory precision (below 0.1°), using the source and known target positions as a reference. The source, in particular, provided a high SNR and being stationary, permitted the averaging of relatively large data sets.

6.2 Contact data processing criteria

Acoustic localization data were checked against GPS data and target log books during the analysis of detection performance of the test system, [2, 3]. Radar tracks were also used to validate contacts against surface shipping. This section reprocesses raw data, substituting detection beam number, sufficient for contact validation purposes, for fine bearing estimation. The latter is obtained by searching the maximum signal in a set of redundantly spaced beams (0.1°). Echo delay and fine bearing measurements are transformed into geographical coordinates taking into account the position of receivers (measured upon mooring them on the sea bottom) and of the transmitters (continuously recorded from DGPS). Better precision can be obtained if receiver drift is continuously recorded. DGPS target data were interpolated to obtain the target position upon reflection of the echo. The effects of the length of the towing cable, depending on depth, speed and direction of the towing boat, was calculated and time delay of echo repeater transmissions were calculated. The Doppler-range ambiguity of the LFM pulses was corrected, taking into account the pulse characteristics and the different Doppler shift of each echo on each receiver in all the different trajectories, (maximum error of 35 m) [7].

The errors between acoustic and DGPS localization are computed ping by ping. The empirical distribution is plotted showing for each error threshold the share of pings, which yielded an equal or better error. The following values are also computed for each run: σ_{LOC} is the RMS value of the errors, $P_{0.5}$ is the 0.5 percentile (the median, i.e. the error threshold, in metres, below which 50% of the data are confined) and $P_{0.8}$ is the 0.8 percentile [8] σ_{LOC} permits a direct comparison with σ_{C_Rao} (Sect. 6.3), while the percentiles provide a more immediate interpretation of results in physical terms, without requiring any hypothesis about the probability density function of the error process.

The SNR of contacts has a strong influence on final precision (Sect. 5.6). To be sure that the strong target strength of the echo repeater was high enough to avoid such effect (and to permit the experimental estimation of other phenomena), the theoretical Cramer Rao lower bound for σ_θ was computed for each contact, ping by ping, taking into account SNR and beamwidth [2]. The σ_θ of each echo was then mapped into the corresponding localization standard deviation σ_{C_Rao}. (Multiple maps as shown in Sect. 5.2 were computed by Monte Carlo simulations for a wide range of σ_θ values, and used as look-up tables). The average σ_{C_Rao} in each run was then computed. An estimate is therefore provided of the effect of SNR on localization performance for each run and receiver (Table 3). The computed σ_{C_Rao} can be compared with the measured σ_{LOC}, run by run.

6.3 Experimental data

This paragraph analyzes the contact localization precision obtained by the experimental DUSS system during the campaign "DUSS'97". Acoustic contacts from the three receivers are compared with DGPS data in a few significant runs performed with an Echo Repeater, with high SNR (mostly above 25 dB at sonar output). Table 3 lists the processed runs and their characteristics.

Table 3 *Summary of runs. Fig. 3 shows target trajectory types "A", "C", "D".*

RUN	Frequnecy kHz	Duration minutes	Source depth m	Target depth m	Target trajectory
0103	3.5	90	110	90	C
0203	3.5	120	110	90	A
0104	3.5	60	110	90	D
0201	1.9	120	80	90	C
0200	1.9	60	80	90	D

Figures 15-1, 15-2, 16-1 and 16-2 show two significant examples of the processed data. The complete set of figures is in Annex B. The figures repeat for each run and receiver the map of the test configuration shown in Fig. 3. In the deployment area (the yellow box), green markers show Receiver 3 (left), 2 (middle), the ship with Receiver 1 and the transmitter (coloured dots from blue to red, showing the limited drifting of the moored ship with time). Acoustic contacts are plotted as coloured dots (blue, green, red for Receivers 1, 2, 3) overlapped on DGPS data (large coloured dots from blue, start of run, to red, end of run). For each run and receiver, the corresponding figure shows the map of contacts (Fig. 15-1 and 16-1) and the empirical distribution of localization errors (Fig. 15-2 and 16-2).

Table 4 below summarizes the characteristics of the runs in terms of σ_{C_Rao} , σ_{LOC}

Table 4 *Summary of localization RMS errors.*

RUN	Frequency kHz	Target trajectory	Duration minutes	Receiver 1 RMS errors σ_{C_Rao} / σ_{LOC} m	Receiver 2 RMS errors σ_{C_Rao} / σ_{LOC} m	Receiver 3 RMS errors σ_{C_Rao} / σ_{LOC} m
0103	3.5	C	90	11/286	7/107	15/146
0203	3.5	A	120	60/652	121/122	176/99
0104	3.5	D	60	5/275	7/144	14/166
0201	1.9	C	120	223/181	252/96	33/193
0200	1.9	D	60	9/176	17/173	28/170

Table 5 summarizes the characteristics of the same runs in terms of $P_{0.5}$ (the median) of errors for Receivers 1-3 individually, run by run, and for the whole data set (left column). $P_{0.8}$ values (the 0.8 percentile) are shown in Annex B. As a term of reference, the target covers 154 m in a minute (from ping to ping).

Table 5 *Summary of localization errors:* $P_{0.5}$.

RUN	Frequency kHz	Target trajectory	Duration minutes	Receiver 1 errors $P_{0.5}$ m	Receiver 2 errors $P_{0.5}$ m	Receiver 3 errors $P_{0.5}$ m	Overall errors $P_{0.5}$ m
0103	3.5	C	90	58	83	99	98
0203	3.5	A	120	353	80	69	78
0104	3.5	D	60	147	125	160	143
0201	1.9	C	120	114	71	116	114
0200	1.9	D	60	142	141	135	147
							Overall $P_{0.5}$ m: **118**

6.4 Comments

In the following discussion the possible sources of localization errors will be divided into two "Groups":

1. Beamwidth and SNR, discussed in Sect. 5.6.

2. All other effects. The main ones are discussed in Sect. 5.1 to 5.5.

The terms σ_{C_Rao} in Table 4 are much lower than σ_{LOC} in most of the runs. The difference between these two variables justifies the hypothesis that the sources of error of Group 2 are dominant. The experimental measurements are therefore representative of the effects on overall system performance of the items listed in Group 2. It is not possible to measure from experimental data, the relative importance of the various contributions within Group 2. The data in Sect. 5 suggest how sensitive the system is to each error source in Group 2. For example, it can be said that the sonar asset positioning errors were certainly known within a standard deviation of about 20 m, that the existing compass biases were certainly compensated within 0.1°, that the error estimating the length of propagation paths was better than 4‰. In fact, each one of these parameter values, alone, would have produced overall localization errors larger than the experimental results obtained.

Only in a few cases, at long range (trajectory type A), or where SNR is lower and the system is very sensitive to bearing errors, are the data strongly related to σ_{C_Rao}.

On the other hand, the measured σ_{LOC}, shown in Table 4, are roughly equivalent to the σ_{C_Rao} corresponding to a SNR of 15 dB, (Sect. 5.6 and Fig. 6b). This means that in the test system used, the system parameters of Group 2 are consistent with the errors generated by Group 1 with a SNR of 15 dB, i.e. upon detection of weak targets with the existing beams. Therefore, in the design of a better system, any improvement in the acoustic apertures (narrower beamwidths) would require concomitant improvements in the other system characteristics.

A few σ_{LOC}. values on Receiver 1, much larger than the average, between 275 m and 650 m, reveal the intervention of exceptional effects. Checks on compass data show that this phenomenon was due to ship's pitching, which induced fast rotation of the array. The slow response of the compass produced these errors. The runs 0103, 0203, 0104 on Receiver 1 are a clear example, confirmed by compass logs.

The maps and percentiles of Table 5 show the localization errors with respect to the DGPS data, which are precise within a standard deviation of 5 m [5]. All $P_{0.8}$ values of individual runs and receivers are better than 225 m, with an overall value of 176 m. $P_{0.5}$ values range from 58 m to 160 m, with an overall median of 118 m for the whole test. Such results can be considered satisfactory lower bounds for the localization of a target within a surveillance range of 20 km and with small receivers.

The comparison of percentiles does not indicate differences between the monostatic and the multistatic receivers. As suggested in Sect. 5.4, the width of separation of the multistatic receivers (e.g. Receiver 3) does not significantly affect their precision.

Receiver beams at 1.9 kHz are half as wide as at 3.5 kHz, yet no evident differences can be found in the results. This fact confirms that in the experiment the error sources of Group 1, beamwidths (7° or 13°) and SNR, were not predominant.

The data of each run span a wide range of conditions due to the movement of the target in a changing environment. They are not sufficiently homogeneous to permit the hypothesis of stationarity, necessary for estimating the probability density of errors. The steep slopes of empirical distribution, and the limited difference between $P_{0.5}$ and $P_{0.8}$, show that errors are concentrated around the median values (Figs. 15-2, 16-2).

The target trajectory type does not significantly affect the results. Target - receiver ranges from 3 to 23 km were tested, in three different trajectory types, but no evident differences among them can be perceived from the results, except Trajectory "D", but available data are not enough to confirm this. In such a trajectory, three different target - receiver ranges are tested at the same time, a fact which does not appear to affect the results.

6.5 Spreading of contacts

The reduced spreading of contacts around the real positions makes it viable to proceed to the fusion of data from each receiver. This permits the creation of an extended system,

consisting of a network of autonomous receiver nodes, where contact detection and localization are improved by the integration of data collected by multiple elements. This section comments on the experimental results obtained during the tests. The spreading of contacts from different receivers is computed ping by ping as the distance of each contact from the barycentre (i.e. the average of positions of the three contacts provided by the three receivers). Plots of the empirical distribution of such spreading are obtained (Annex C). The median of overall spreading is also computed for each run. These data provide an input to a discussion of the feasibility of merging objects independently detected and localized by each multistatic node. It is also possible to derive indications on the minimum width of spatial windows required for merging contacts into a single object. This parameter is important for estimating the expected processing overhead of data fusion algorithms: the wider the acceptance windows, the more associations among contacts the system has to process. Too large a window requires an impractical level of computing resources.

Table 6 *Median values of contact spreading around the barycentre. (*): Receiver 1 not included. More data are listed in Annex C.*

RUN	Frequency kHz	Target trajectory	Duration (minutes)	Contact Spreading $P_{0.5}$ [m]
0103	3.5	C	90	60
0203	3.5	A	120	50
0104	3.5	D	60	60
0201	1.9	C	120	70
0200	1.9	D	60	62

The percentile values summarized in Table 6 show that most contacts are spread within a limited range of each other, with a maximum $P_{0.5}$ of 70 m. More data are shown in Annex C. Typical values for $P_{0.8}$ of 110 m were found. A similar contribution to the spreading of contacts can be expected from errors of Group 1, i.e., from a lower SNR (15 dB) interacting with the beamwidth. The σ_{C_Rao} values computed for this SNR were found to be roughly equal to the σ_{LOC} (Table 4) and the RMS spreading (Annex C, Table C1) of the experimental data. With a 200 Hz FM pulse and 7° beam, this limit is well within one beamwidth for ranges exceeding 1 km and corresponds to 30 independent range cells. In spite of the limited size of receivers, the imperfect moorings and compasses, the potential for efficient fusion of contacts is demonstrated.

6.6 Advantages of contact fusion.

In an operational situation, the target position is not known, and localization data from different receivers must be merged. The displacement of the "barycentre" (i.e. the averaged position of the three contacts from the three receivers) from the DGPS position

of the target is estimated for each ping. Percentiles and empirical distributions are computed. This is a simplified representation of the potential target localization improvements obtained with the fusion of data from several receivers. The average of data from the three receivers with equal weighting is justified by the uniformly high SNR of contacts from the echo repeater.

This approach is representative of a distributed system by which contacts are detected and localized on each autonomous receiver, thus reducing the flow of data to a central node, which subsequently performs the merging and classification of targets.

Table 7 *$P_{0.5}$ percentiles of errors after "data fusion" (errors between barycentre of contacts from the three receivers and DGPS target positions) are compared to overall $P_{0.5}$ before that (errors between contacts and DGPS positions) for each run.*

RUN	Frequency kHz	Target triage.	Duration minutes	Overall $P_{0.5}$ of individual receivers errors, m	Error after contacts merging, $P_{0.5}$, m	Difference%
0103	3.5	C	90	98	79	24%
0203	3.5	A	120	78	68	14%
0104	3.5	D	60	143	151	- 5%
0201	1.9	C	120	114	79	44%
0200	1.9	D	60	147	126	17%
						average: 22%

Noisy data from Receiver 1 were included in the computations, with the exception of Run 0203, Receiver 1. A significant improvement from merging is evident in these results. The average of 22% is weighted by the number of pings of each run. More sophisticated and realistic algorithms, taking into account the extended aperture of the multistatic field and the different degree of confidence of asset positions, contact delay and bearing, would achieve better results.

6.7 Design criteria

The experimental data analyzed, yield satisfactory results in terms of contact localization precision and inter-receiver information fusion. They are representative of the system characteristics of Group 2 (Sect. 6.4). It has also been shown in Sect. 5.4 that wider deployment patterns do not amplify the effect of these error sources. The specification of a new DUSS should reflect such characteristics.

An overall maximum bias of 0.1° is required for the bearing measurement precision of receivers, including the effects of hydrophone frame deformations, compass

characteristics and coupling to the array, magnetic declination compensation. A post - deployment calibration procedure can achieve satisfactory results by means of the known position of the acoustic source.

An overall maximum bearing standard deviation of 0.1° is also required. It can be achieved with very low - noise digital compasses having at least a 10 bit A/D quantization. A minimum sampling frequency of 1 Hz is recommended. More bits, faster sampling coupled with filtering techniques can reduce the white noise component in the compass measurements.

The hydrophone frame must be rigid enough to respect the above requirements, and must include a fin to avoid rotation of the array. The dynamic response of the compass needs to be compatible with the residual rotation rate.

The deployment location of receivers must be known within a maximum bias and variance of 20 m. The inherent precision of a DGPS system is satisfactory (5 m standard deviation). Particular care is required to reduce or estimate the displacement between the array and the floating DGPS antenna within the specification above.

The beamwidth of receivers is critical with low SNRs (barely detectable targets). As shown in Sect. 5.6, a given beamwidth and SNR correspond to a target localization error with a standard deviation σ_{C_Rao} linearly increasing with target - receiver range; the maximum reached at 20 km range is used as a reference in the table below.

Table 8 *Target localization error*

Beamwidth	SNR	σ_{C_Rao} at 20 km
13°	15 dB	450 m
7°	15 dB	250 m
7°	10 dB	450 m
4°	10 dB	250 m

A beamwidth of 7° with a SNR of 15 dB yields a performance which is roughly equivalent to the σ_{LOC} of the experiments. It can be assumed as a specification for an operational DUSS if the results of the present experiments are judged satisfactory. The same 7° beam with a SNR of 10 dB, yields a σ_{C_Rao} of 450 m at 20 km. On the contrary, a beamwidth of 4° is recommended if σ_{C_Rao} is to be kept below 250 m at 20 km ranges with a SNR as low as 10 dB.

The most critical item in the definition of a specification for receiver beamwidths is the size of the contact association windows of data fusion functions. Such window sizes depend on the efficiency of the algorithms adopted, the available computing power, the number of false alarms and the extent of the area surveyed. The present specifications (7° and 4°) are intended to limit the spreading of contacts to less than 100 independent sonar

pixels. It is not possible in this phase of the study to estimate the corresponding overheads and problems in real data fusion algorithms, nor to define a system specification more precisely tailored to such issues. It should however be noted that if receiver characteristics allow successful data association, the overall localization precision of the multistatic DUSS network can be considerably better than that provided by each receiver.

7 Conclusions

This study analyzes the contact localization potential and experimental performance in shallow water of a Deployable Underwater Surveillance System. The feasibility of data fusion across multiple receivers and the corresponding gain in localization precision at surveillance ranges up to 20 km are also discussed..

The main sources of localization errors in a multistatic sonar system are considered, and the sensitivity of the system to such parameters is evaluated with simple models. The sources of error are divided into two Groups:

1. Beamwidth and SNR.

2. Other effects: compass precision, hydrophone frame, localization of deployed sonar assets, sound propagation delays, wavefront distortion.

450 pings collected with three receivers at 1900 and 3500 Hz along 3 types of target trajectory are processed and summarized. Localization errors are computed in terms of the median of displacement between acoustically localized contacts and the corresponding DGPS target position. A median between 58 m and 160 m was found in the 5 target runs examined, with an overall value of 118 m for the whole test. The results do not reveal a significant dependence on monostatic/multistatic receiver, source - receiver deployment distance, target trajectory type, target range (between 3 and 23 km), working frequency or receiver beamwidth.

The experimental results are primarily representative of the effects of Group 2, thanks to the high SNR of the echo repeater target. From the comparison of these results and the models, a specification of some system parameters can be inferred:

- Bearing measurement: maximum bias and standard deviation 0.1°, including compass quantization and noise, assembly precision and hydrophone frame rigidity.
- The compass and the processing of its data need to respond without errors to rotations of up to 1°/min. The beamformer needs to update beam directions accordingly, at least 10 times per min to be compatible with the 0.1° specification above.
- Knowledge of deployment position: maximum bias and standard deviation 20 m.
- DGPS precision: maximum bias and standard deviation 5 m.
- Synchronization of multistatic assets: precise within a few sampling intervals (at the sampling frequency required by the bandwidth of the basebanded pulse).

- The length of underwater acoustic paths must be known within a maximum approximation of 4‰.

Particular care is needed to avoid biases in the compass. A post-deployment procedure to calibrate residual bias using the acoustic source as a reference should always be considered. A rigid hydrophone frame is required to accomplish the above requirements. A fin is recommended to reduce receiver array rotations. The beamformer re-computes beam directions during the processing of a ping to compensate the residual rotations. Noise in the compass measurements must be filtered out. Deployment positioning accuracy is another critical issue. Differential GPS measurements proved to be precise enough. Wide multistatic configurations do not unduly amplify asset positioning errors. Nonetheless, drifting and deployment uncertainty of moorings and tilting of cables may affect results with maximum errors (bias and standard deviation) of 70 m, which can be corrected by means of dedicated floating Differential GPS buoys connected to the receivers. Displacements of the differential GPS antenna from the submerged arrays, however, can still represent a severe limitation to system performance, to be countered with a proper mechanical structure. Additional sensors can be considered to estimate such displacement. The experimental data and models considered here suggest limited influence on the results of environmental effects such as propagation path length and wavefront distortion. This hypothesis is supported by the shallow depth and high sound absorption of the bottom in the test site, the moderate ranges of the target and the small acoustic apertures of receivers.

The localization errors of the three independent receivers determine the scattering of received contacts. In each ping, the centre of the three detected contacts was determined, and its distance from each individual echo was analyzed. The resulting median is always below 110 m, which corresponds to an extension of 30 range - bearing independent cells. Again, no particular dependence on such test conditions as frequency, target trajectory, monostatic/multistatic geometry is evident. An average improvement of contact localization precision of 22% is demonstrated after fusion of contacts with a very simplified method. Further benefits are provided by receiver diversity with real targets, due to their aspect dependent echoes and independent fading at different times on the different receivers.

The localization errors corresponding to Group 1 items were estimated for various beamwidth and SNR hypotheses by means of Cramer Rao formulae. Such errors were discussed using the experimental results described above as a term of reference. Specification of a 7° beamwidth corresponds to errors equivalent to the performance of experiments with a minimum echo SNR of 15 dB. A smaller beamwidth of 4° is required for a SNR of 10 dB (if barely detectable targets have to be localized with the same accuracy of the experiments). These values correspond to an estimated size of up to 100 independent range - bearing cells for the contact association windows of data fusion algorithms.

8 Recommendations

The problem of precise mooring of the assets deserves careful attention. A DGPS device only partially resolves the problem. The displacements between the floating buoy and the submerged array must be countered with a proper mechanical structure or estimated with additional sensors. Improvements in compass performance appear feasible. The performance of complete data fusion algorithms needs to be tested, in order to finalize specifications on beamwidths, which have a strong impact on receiver size and complexity. The present results should be taken into account for the design of the prototype. Further study of contact localization performance enhancement is recommended.

9 References

[1] Mozzone, L., Bongi, S. Deployable underwater surveillance systems - analysis of experimental results, SACLANTCEN SR-278. La Spezia, Italy, NATO SACLANT Undersea Research Centre, 1997.

[2] Mozzone, L. , Bongi, S. , Primo, F., Deployable underwater surveillance systems - analysis of experimental results. Part II, SACLANTCEN SR-283. La Spezia, Italy, NATO SACLANT Undersea Research Centre, 1998.

[3] Mozzone, L. , Bongi, S. Deployable underwater surveillance systems - analysis of experimental results. Part III, SACLANTCEN SR-288. La Spezia, Italy, NATO SACLANT Undersea Research Centre, 1998.

[4] Chen, C.H. editor. Signal Processing Handbook. New York, M. Dekker, 1988: Paragraph 3.1. [ISBN 0-8247-7956-8].

[5] Installation and operation manual for model 3009/3012 differential GPS receiver. Del Norte technology Inc.

[6] Burdic, W. Underwater acoustic system analysis, Prentice-Hall., 1991: Paragraph 13.3.3. [ISBN 0-13-947607-5].

[7] Nielsen, R. O. Sonar signal processing, Artech House, 1991, Paragraph 5.2.3 [ISBN 0-89006-453-9]

[8] Papoulis, A. Probability, Random variables and stochastic processes, McGraw - Hill, 1991. Paragraph 4.2. [ISBN 0-07-048477-5].

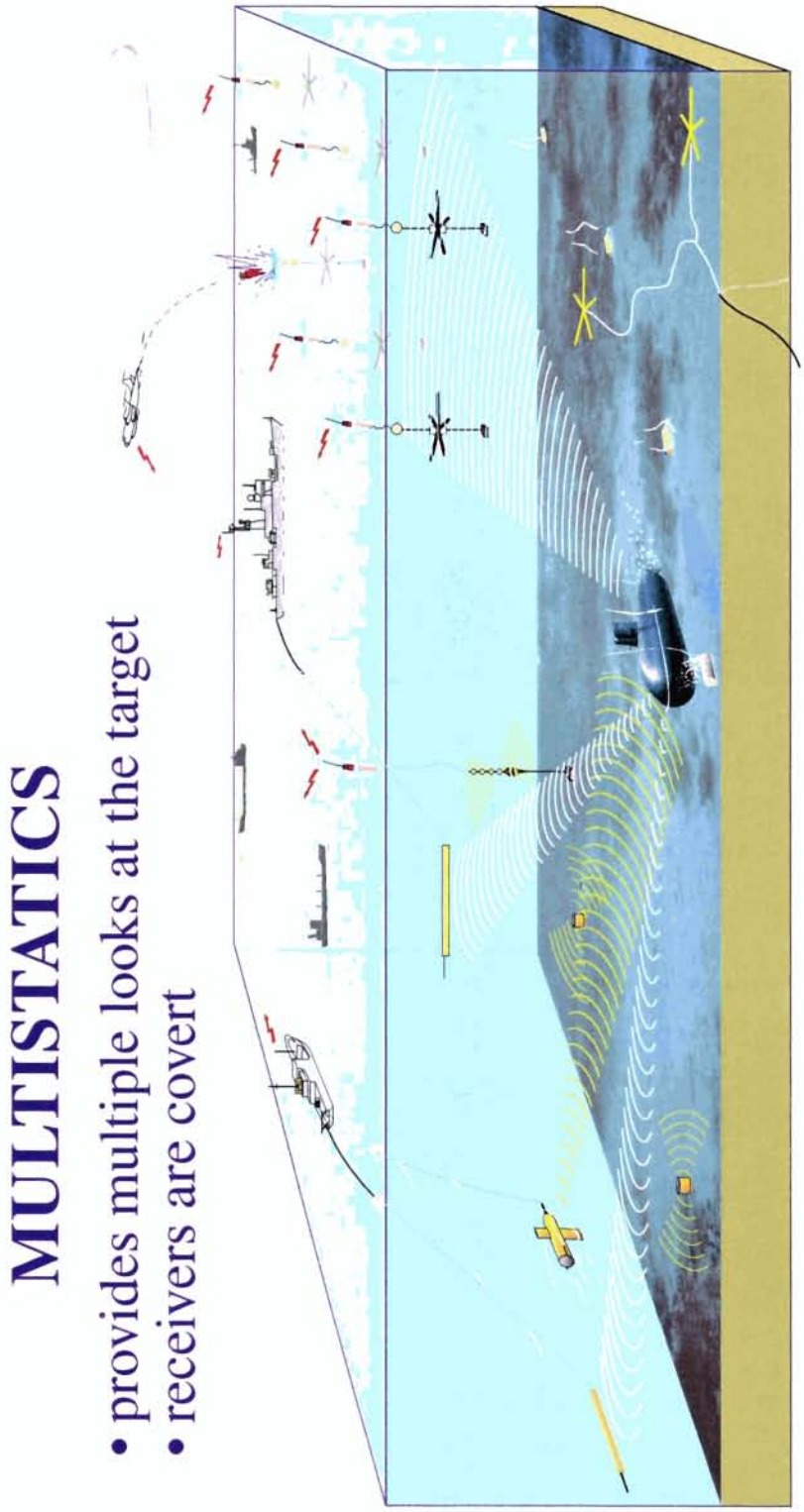

Figure 1 *Pictorial view of the DUSS concept.*

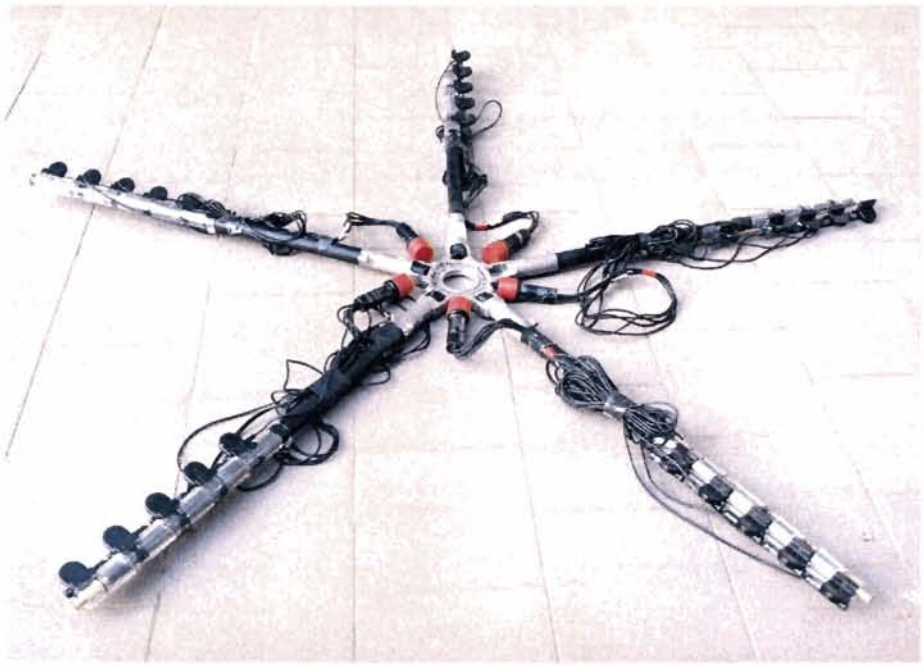

Figure 2 *Picture of receiver hydrophone frame.*

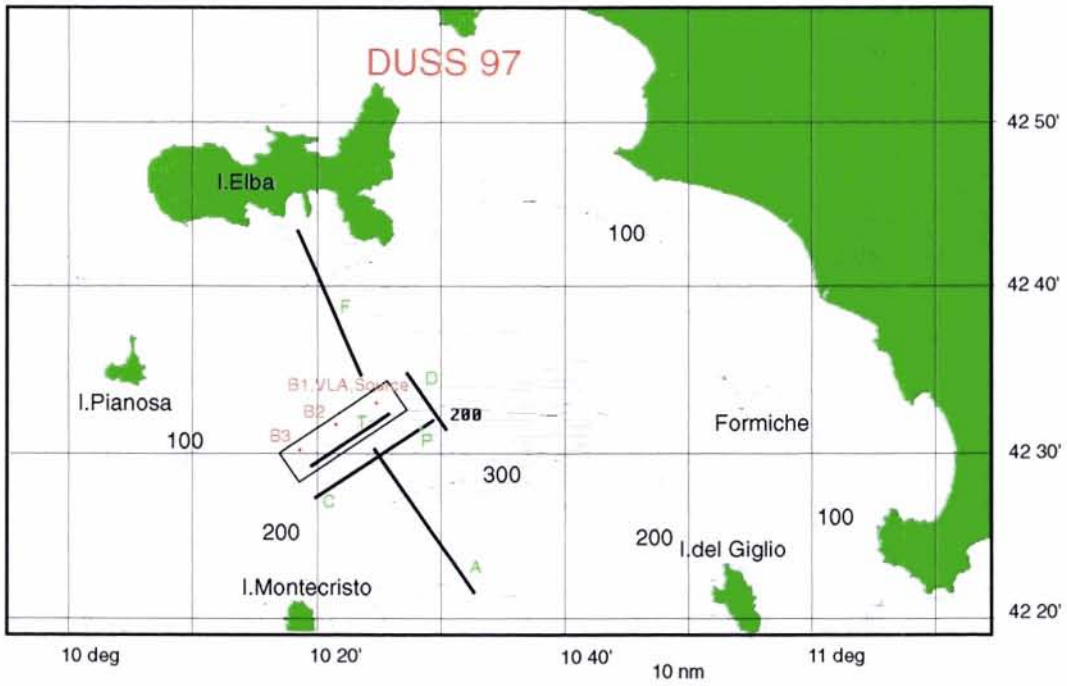

Figure 3 *Geographical map of the test area, showing bottom bathymetry and deployment positions of sonar elements. The box indicates the restricted area for assets deployment. Target trajectories (A, C, D) are shown.*

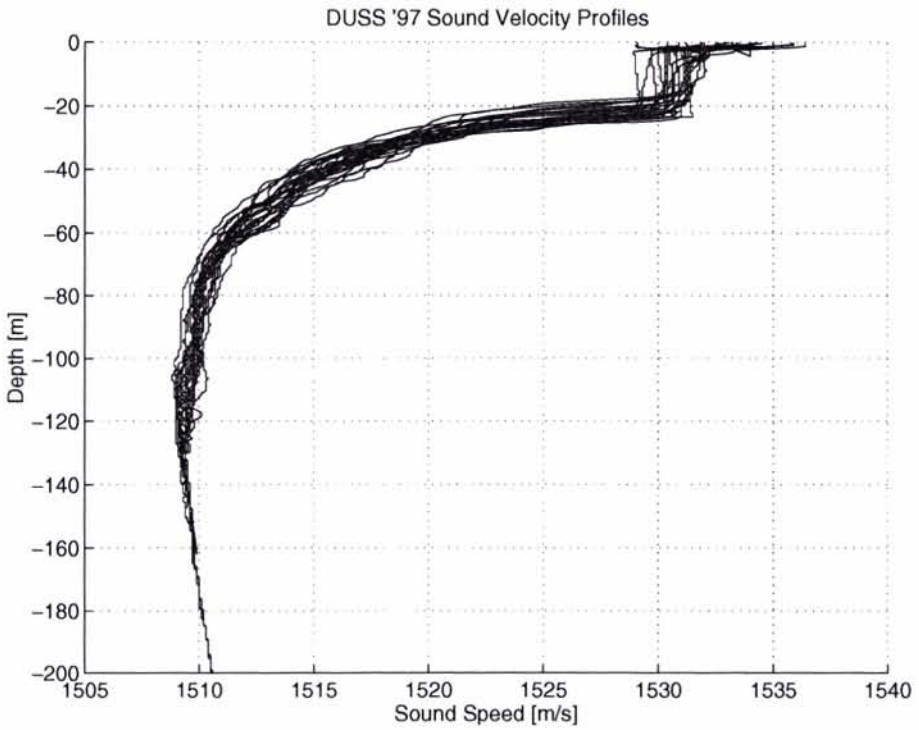

Figure 4. *Sound velocity profiles measured during the tests.*

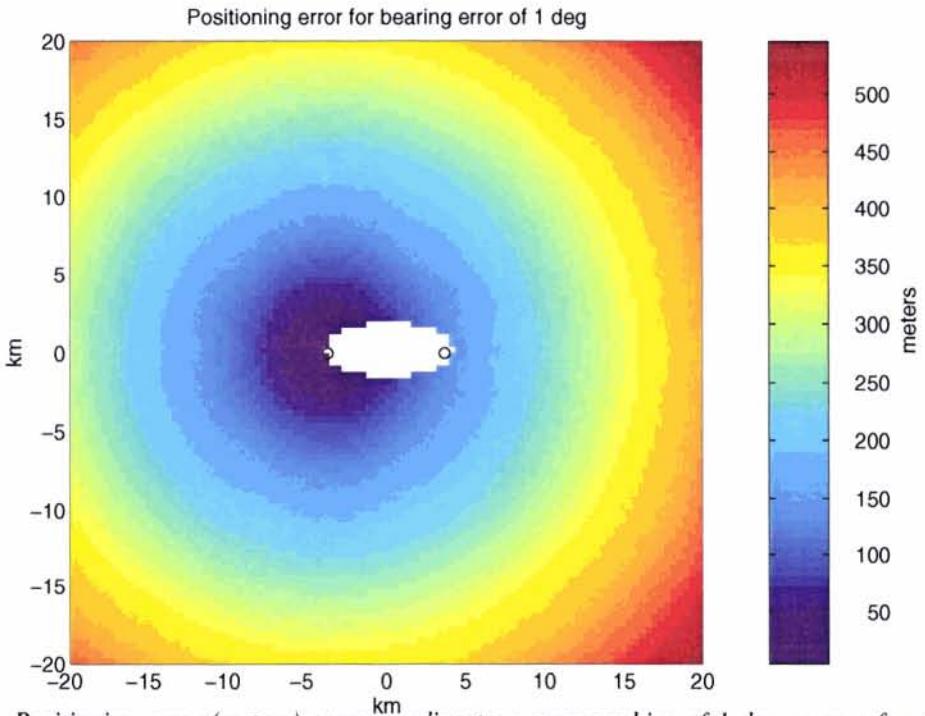

Fig. 5. *Positioning error (meters) corresponding to a compass bias of 1 degree as a function of contact position on the geographical map. Also the positions of transmitter(circle on the right side) and receiver (circle on the left side) are shown.*

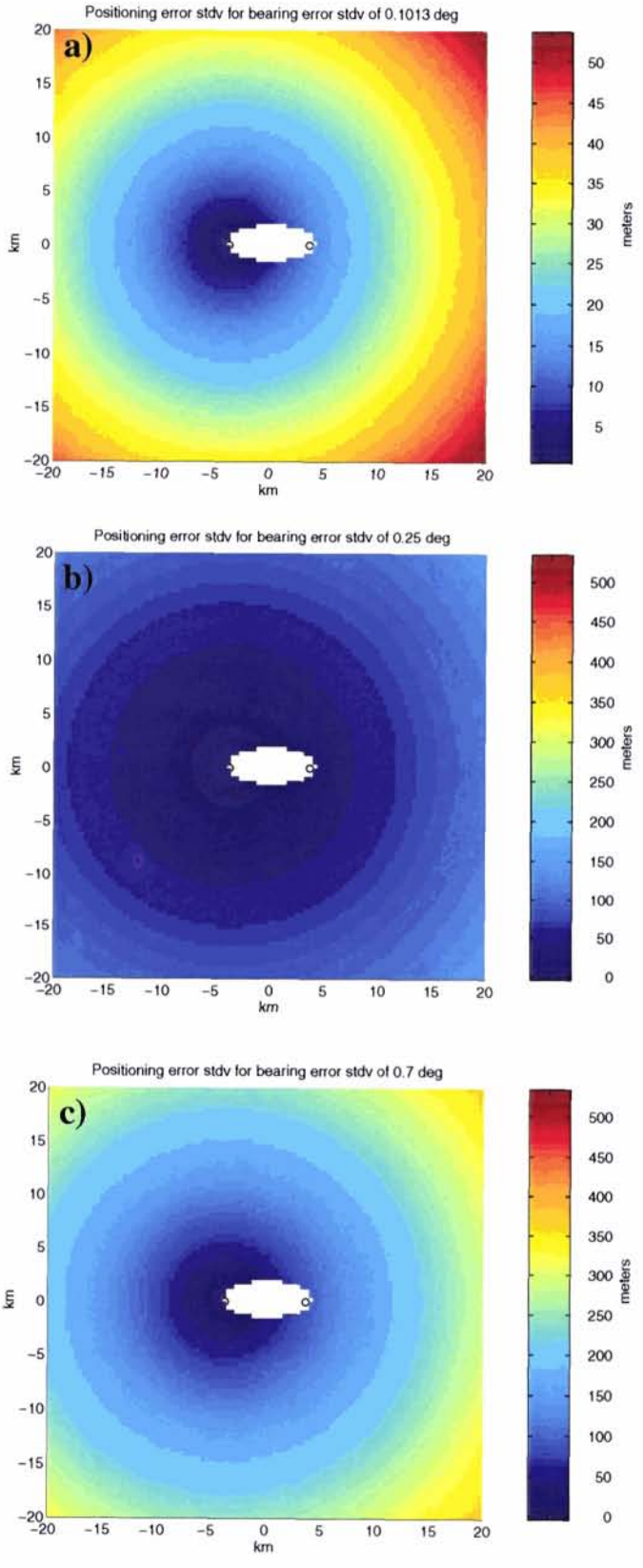

Figs. 6a ... 6c. *Contact localization error due to random bearing error with standard deviation values of 0.1° (effect of receiver compass quantization), 0.25°, 0.7°. The standard deviation of error (RMS error, meters) is shown for all possible positions of the contact in the geographical map. Also the positions of transmitter(circle on the right side) and receiver (circle on the left side) are shown.*

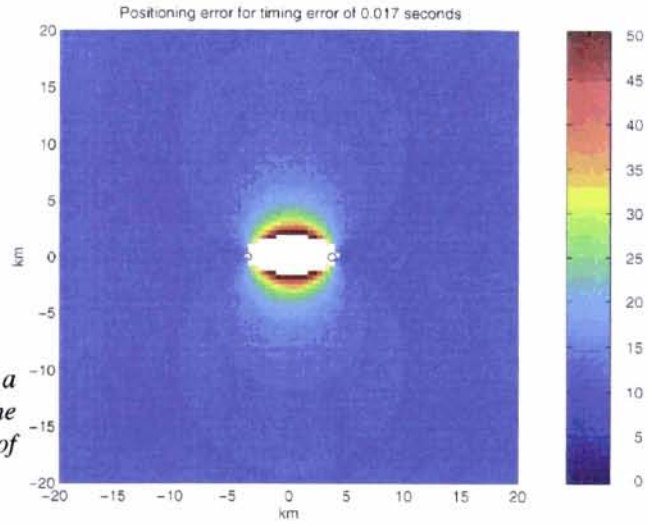

Fig. 7. *Contact positioning error as a function of actual contact position on the geographical map for a timing error of 17 ms.*

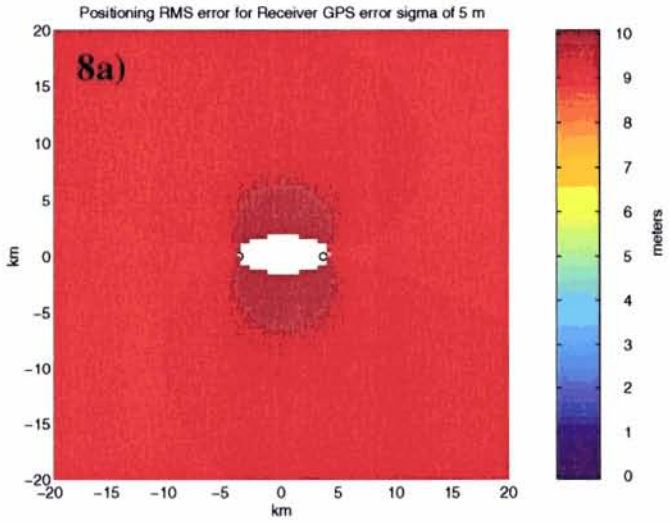

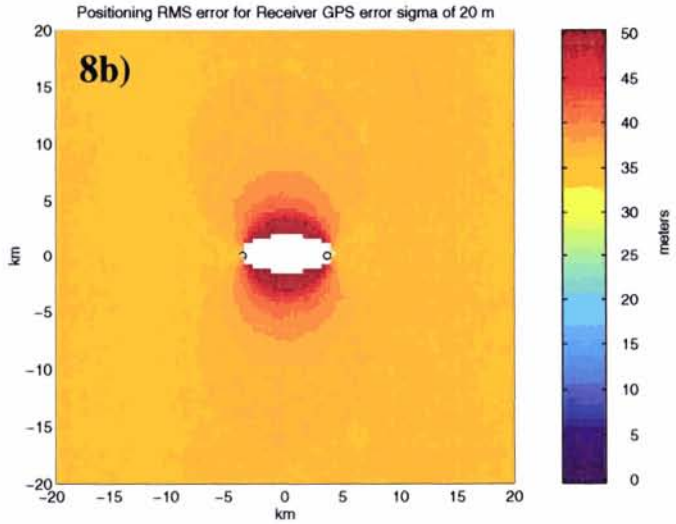

Figs. 8a, 8b. *Contact localization RMS error versus actual contact position on the geographical map. An RMS error of 5 m (Fig. 8a) and 20 m (Fig. 8b) is assumed in the knowledge of the receiver's position.*

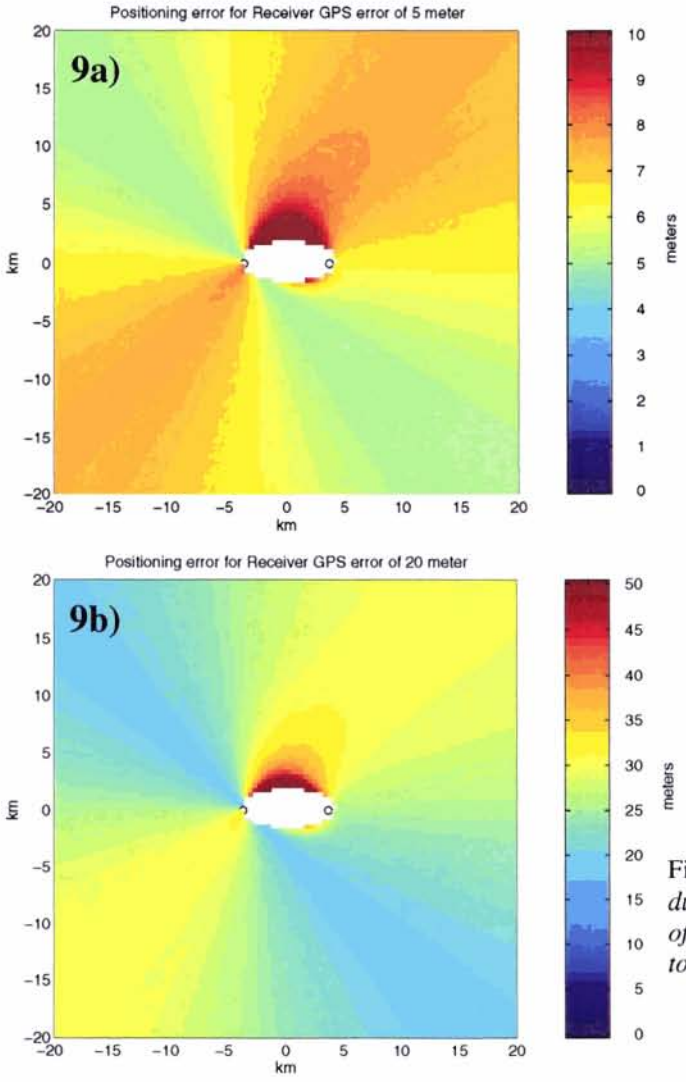

Fig. 9a, 9b. *Contact localization bias due to unwanted drifting of the receiver of 5 m (Fig. 9a) and 20 m (Fig. 9b), towards North-West.*

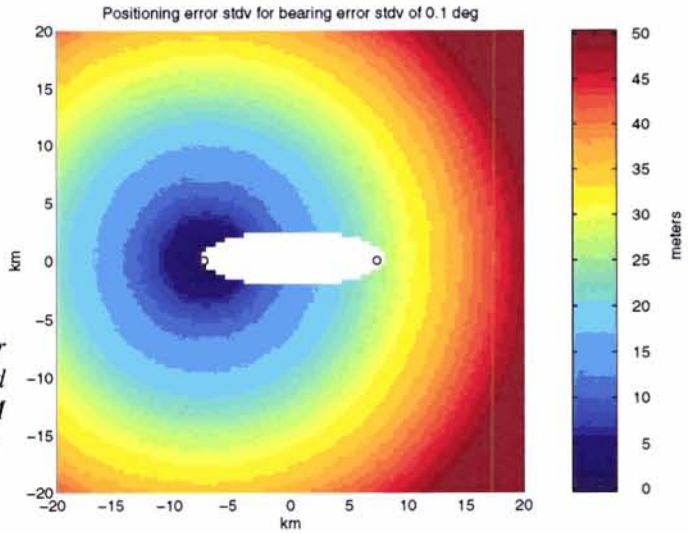

Fig. 10. *Contact localization RMS error due to bearing error with standard deviation of 0.1 degrees and 8 NM distance between source and receiver.*

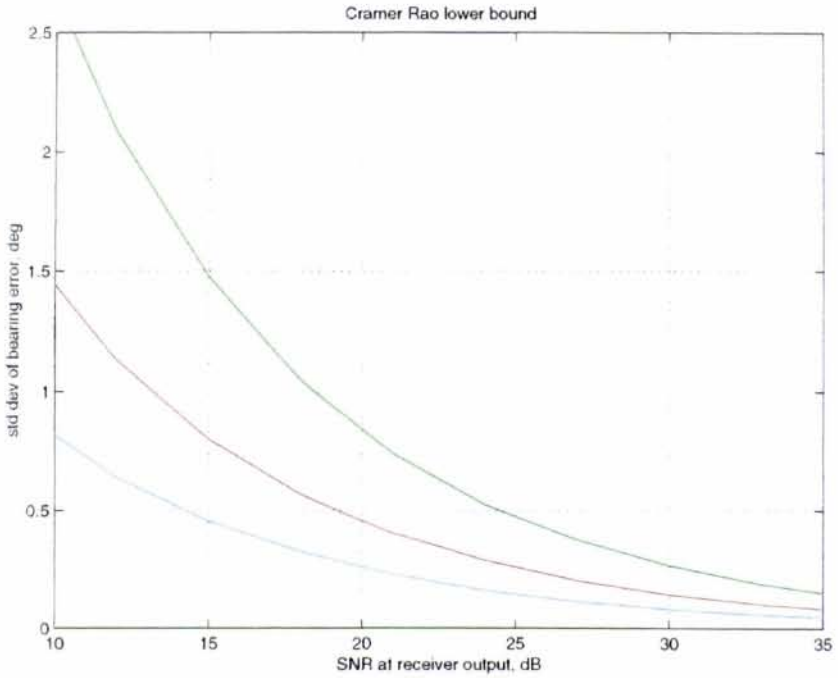

Fig. 11. $\sigma\theta$ *with 13° beam (1.9 kHz, green line), 7° beam (3.5 kHz, red line), 4° beam (not tested in experiments, blue line) versus SNR at receiver output.*

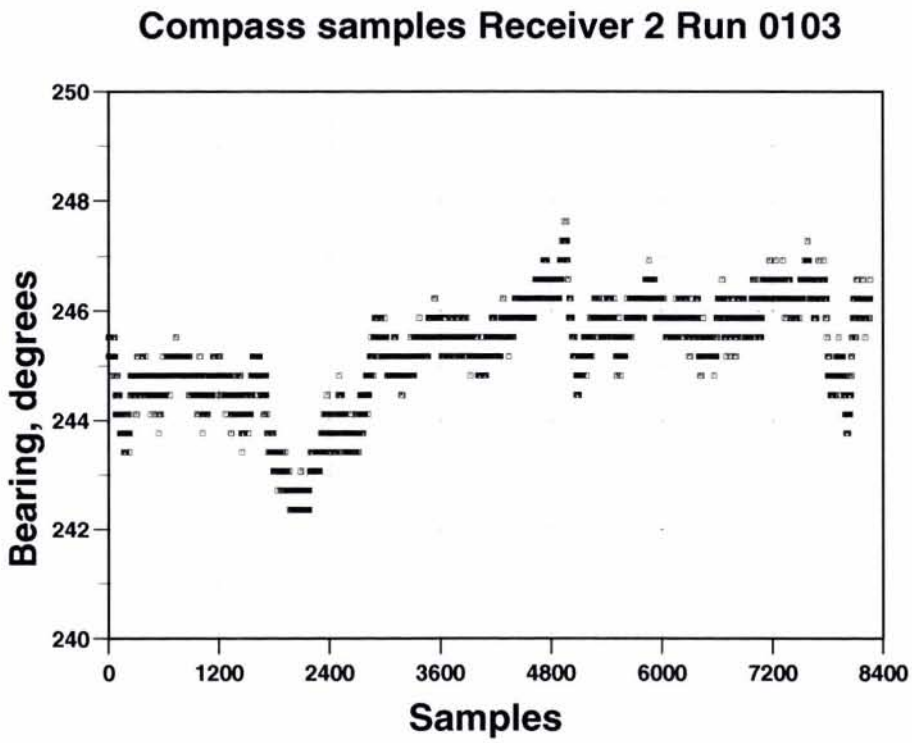

Fig. 12. *Compass time series during a typical run. Quantization steps are visible. Sampling frequency is 1 Hz*

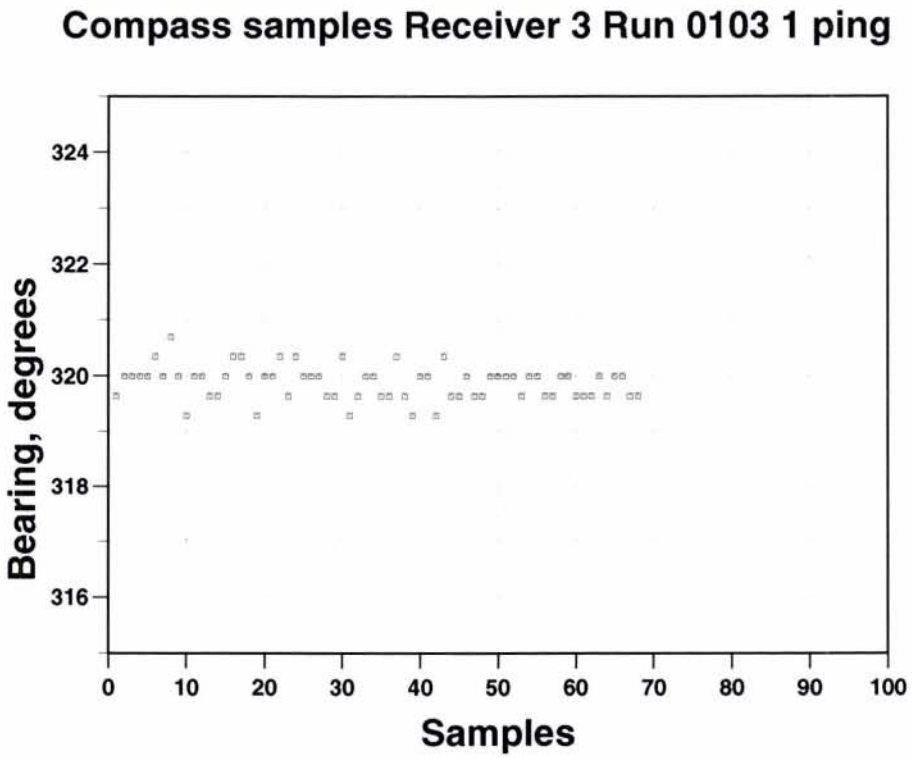

Fig. 13. *Compass time series during a typical ping interval (1 minute), with little array rotation. The presence of noise is visible.*

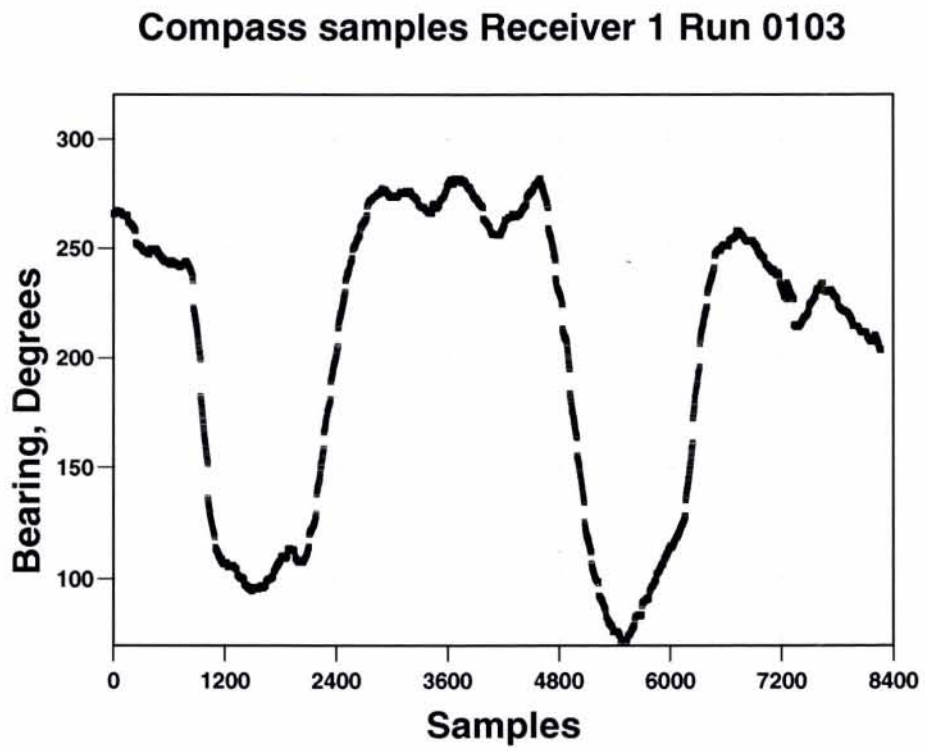

Fig. 14. *Compass time series during an abnormal ping, with rapid compass changes; slow compass response produces bearing errors.*

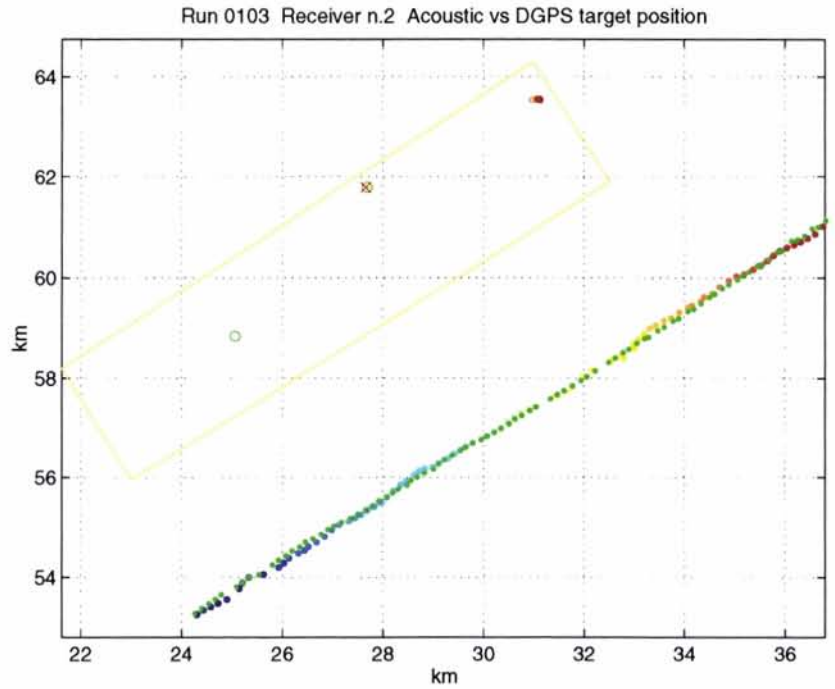

Figure 15_2. *Run 0103, 3.5 kHz, Trajectory C, Receiver2. Empirical distribution of contact localization erros.*

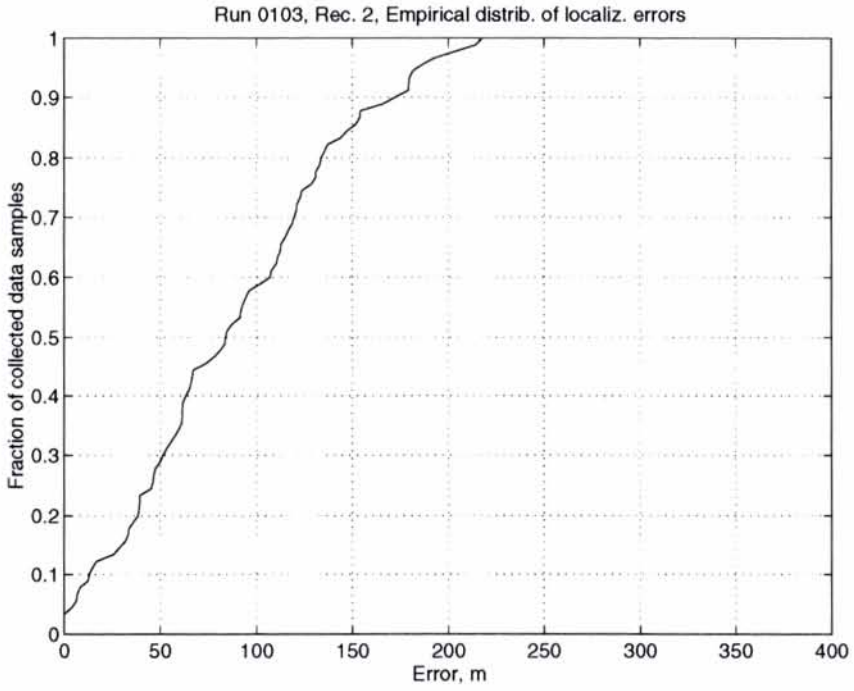

Figure 15_1. *Run 0103, 3.5 kHz, Trajectory C: acoustic contacts from Receiver 2(green dots) and GPS trajectory (color dots).*

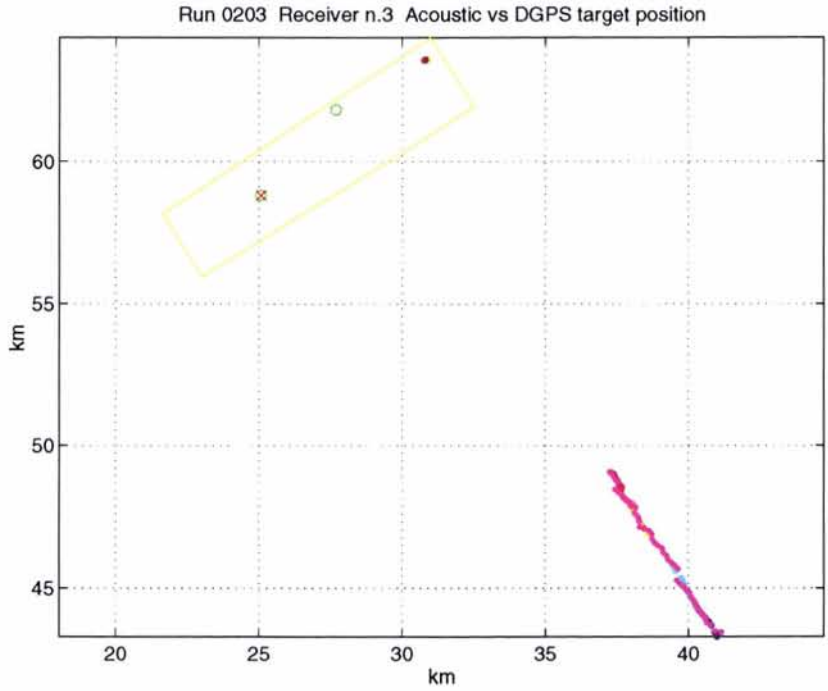

Figure 16_1. *Run 0203, 3.5 kHz, Trajectory A: acoustic contacts from Receiver 3(magenta dots) and GPS trajectory (color dots).*

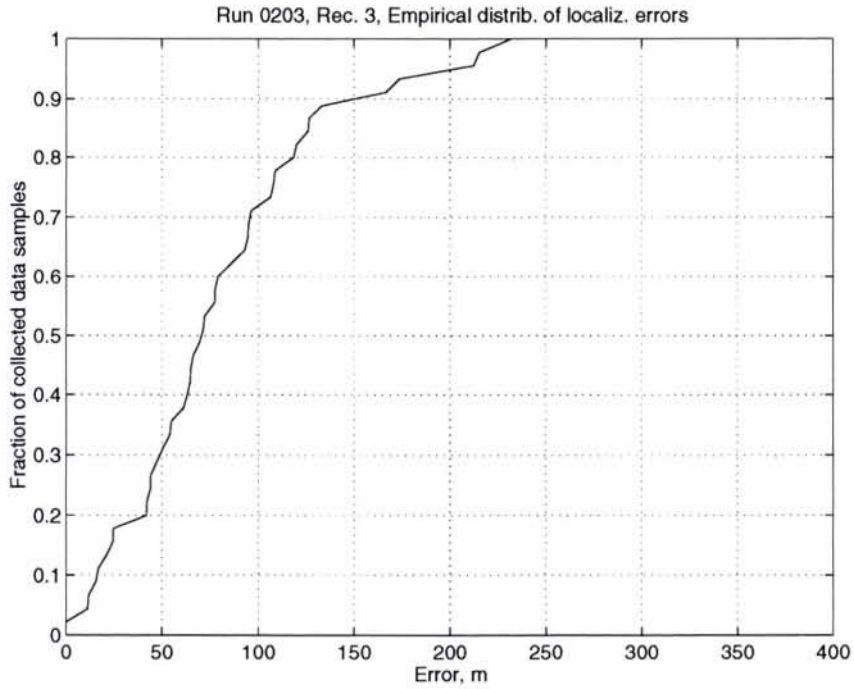

Figure 16_2. *Run 0203, 3.5 kHz, Trajectory A: acoustic contacts from Receiver 3. Empirical distribution of contact localization erros.*

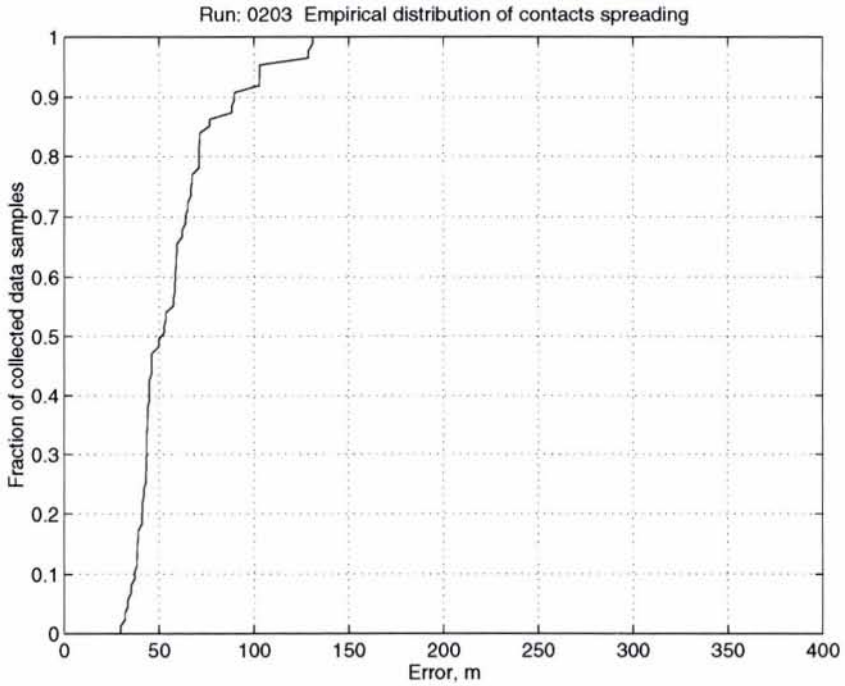

Figure 17. *A significant example of empirical distribution function of contact localization spreading (Run 0203). More plots are shown in Annex C.*

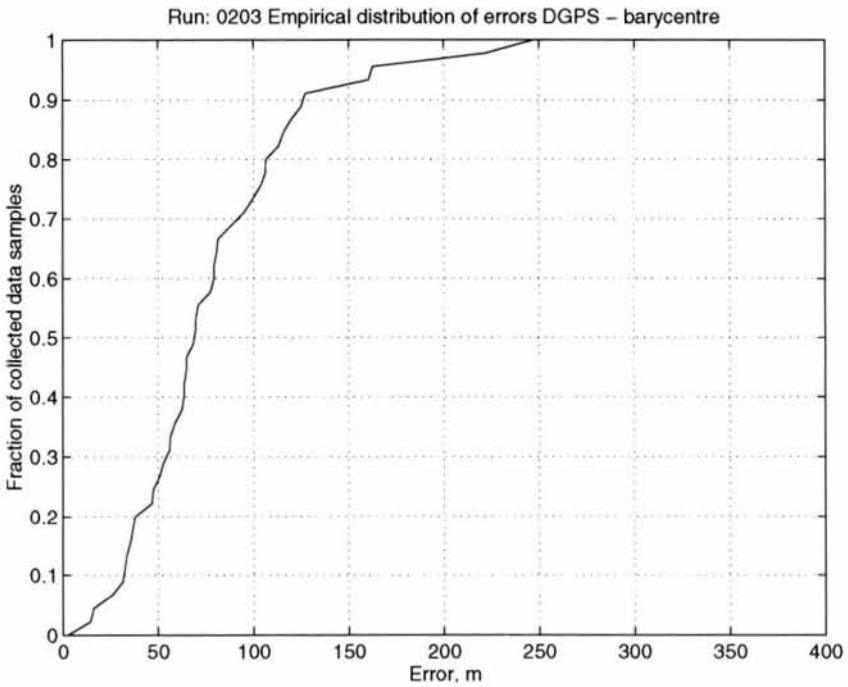

Figure 18. *Run 0203. Empirical distribution of errors between barycentre of contacts from the three receivers and DGPS target position.*

Annex A - The experimental sonar system

1900 Hz Transmitter: SL = 204 dB, 200 Hz bandwidth, 10 elements at 0.5 lambda, no shading is used. Max. depth: 90 m. It is battery powered and activated *via* radio. During the tests it was hanging overboard while the ship was kept on station.

3.5 kHz Transmitter: SL = 205.5 ±2.5 dB, 200 Hz bandwidth, 5 elements at 0.5 lambda. It was coupled to the transmitter above.

Table A1 *Source Levels and -3 dB vertical beam widths in degrees.*

Frequency	Source Level	Vertical Beamwidth
1900 Hz	204 dB	10.5°
3500 Hz	205.5 ± 2.5 dB	20.8°

Receivers: 25 calibrated hydrophones, star shaped. The length of the arms was tuned for best performance in the three bands above. The receivers were moored to the bottom (80 m depth), battery powered, and transmitted base banded data *via* radio link to *Alliance*. They are triggered by transmitter pulse to work on a band of +/- 120 Hz for 50 s, after which they return to stand-by mode. They include a compass to allow beamforming relative to the North.

Table A2 *Shows -3 dB Beam widths in degrees, DI and horizontal Array Gain (AG_H) in dB:*

Frequency	Horizontal	Vertical	DI	AG_H
900 Hz	28.1°	81.6°	10.5 dB	9.8 dB
1900 Hz	13.2°	54.6°	13.3 dB	12.5 dB
2700 Hz	9.3°	46.4°	13 dB	11.4 dB
3500 Hz	7.1°	40.7°	12.9 dB	11.3 dB

Positioning: Positions and trajectories of all participating elements, including shipping traffic and sonar moored assets, are measured with GPS or radar and stored. They are vital for reconstruction of the multistatic geometry of the experiments. A system named RELAPS allows real time transmission of the position of a remote ship or sonar *via* radio to *Alliance*.

Processing: While data from receivers are stored on Exabyte tape, signals are processed in real time by general purpose Alpha workstations, where beam forming, replica correlation and display processes are performed.

Annex B - Contact localization data

Table B1 *Summary of localization errors:* $P_{0.8}$.

RUN	Frequency kHz	Target trajectory	Duration minutes	Receiver 1 errors $P_{0.8}$ m	Receiver 2 errors $P_{0.8}$ m	Receiver 3 errors $P_{0.8}$ m
0103	3.5	C	90	170	134	156
0203	3.5	A	120	689	156	119
0104	3.5	D	60	427	177	199
0201	1.9	C	120	217	123	224
0200	1.9	D	60	204	208	205

This annex shows all the plots described in Sect. 6.3. The plots are referred to Receivers 1 (top of page, blue dots) to 3 (bottom, red dots). The plots on the left show the geographical map of contacts. The plots on the right show the empirical distribution of errors.

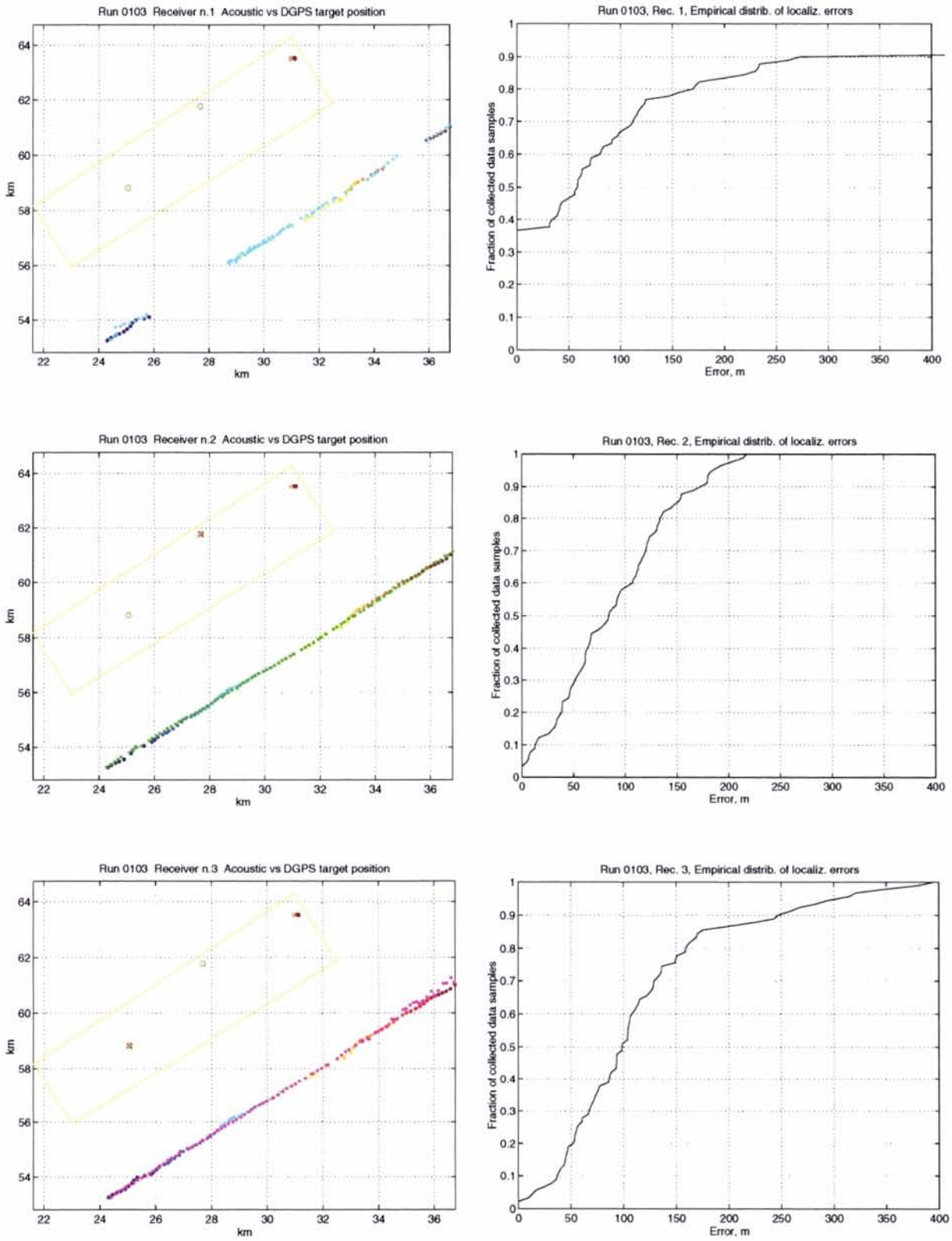

Figure B1. *Run 0103, 3.5 kHz, Trajectory C, Receiver 2.*

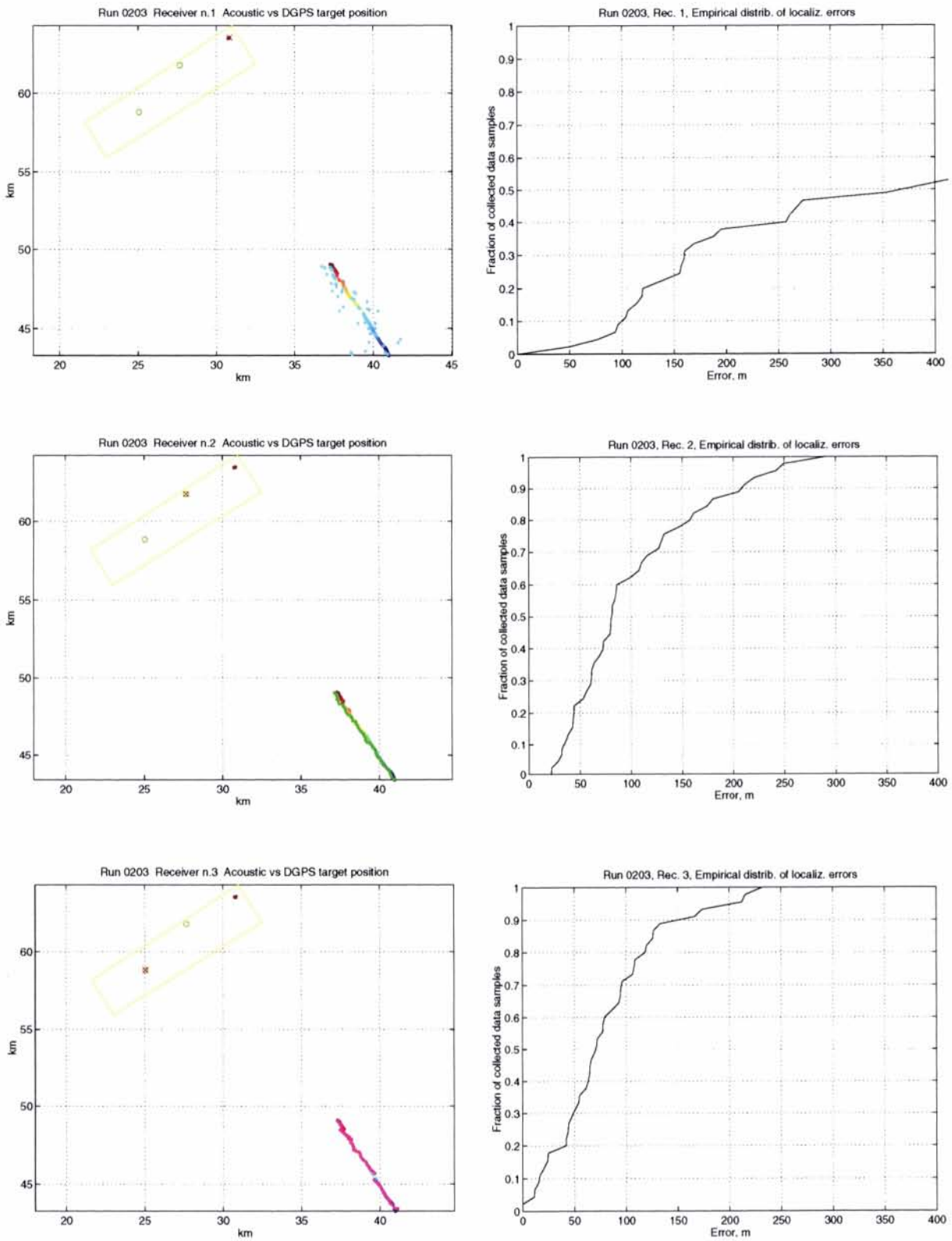

Figure B2. *Run 0201, 1.9 kHz, Trajectory C, Receiver 2.*

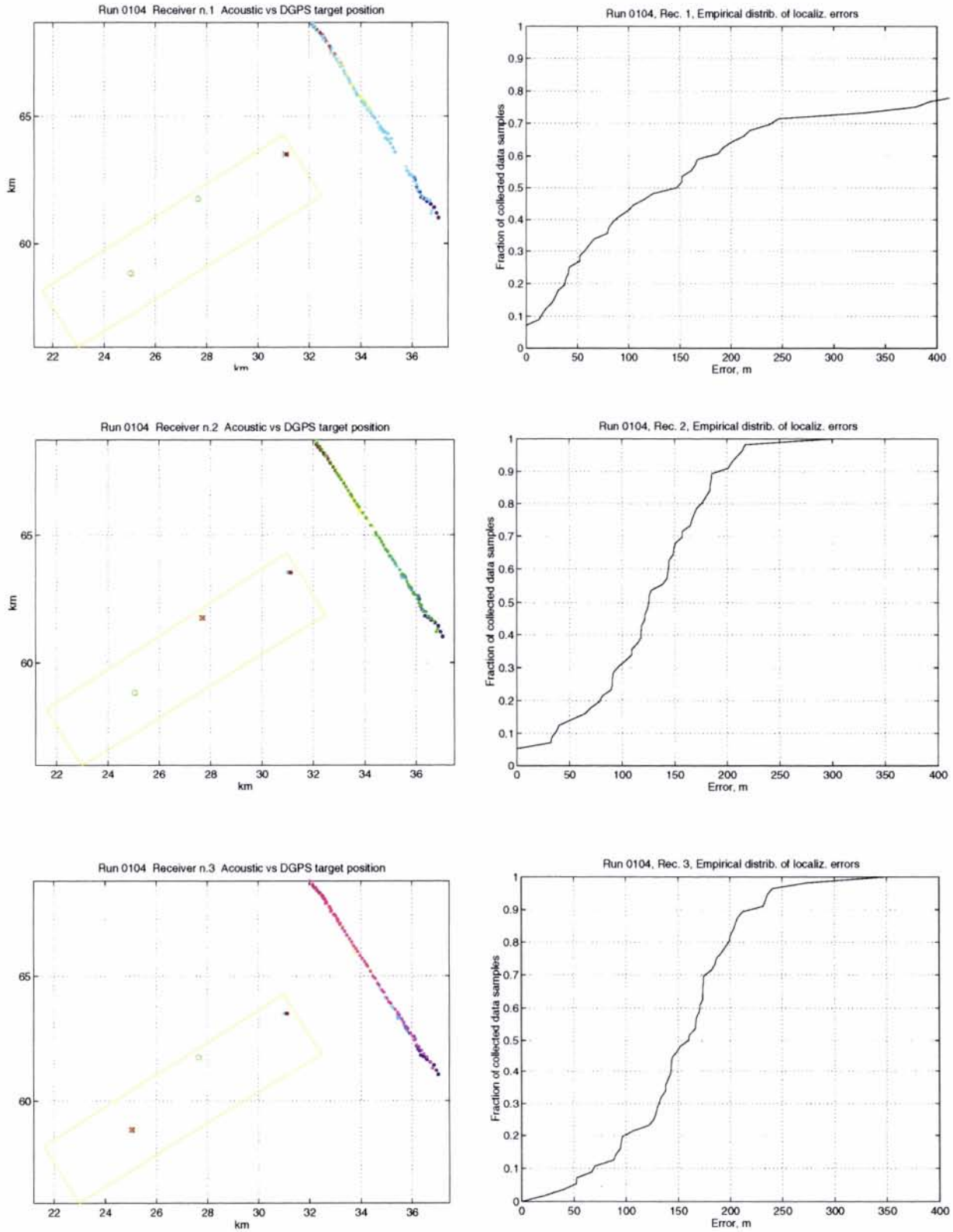

Figure B3. *Run 0203, 3.5 kHz, Trajectory A, Receiver 2.*

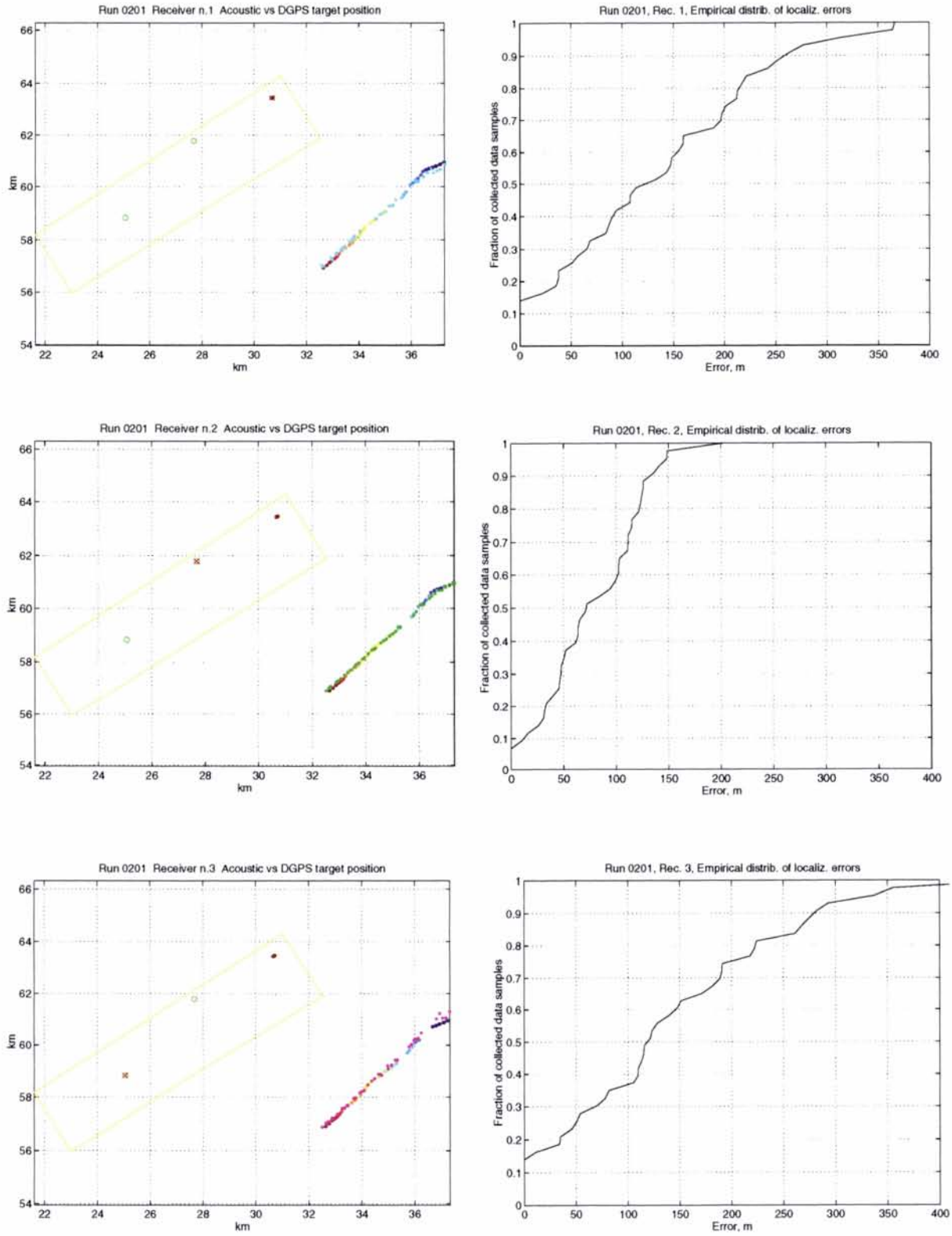

Figure B4. *Run 0104, 3.5 kHz, Trajectory D, Receiver 2.*

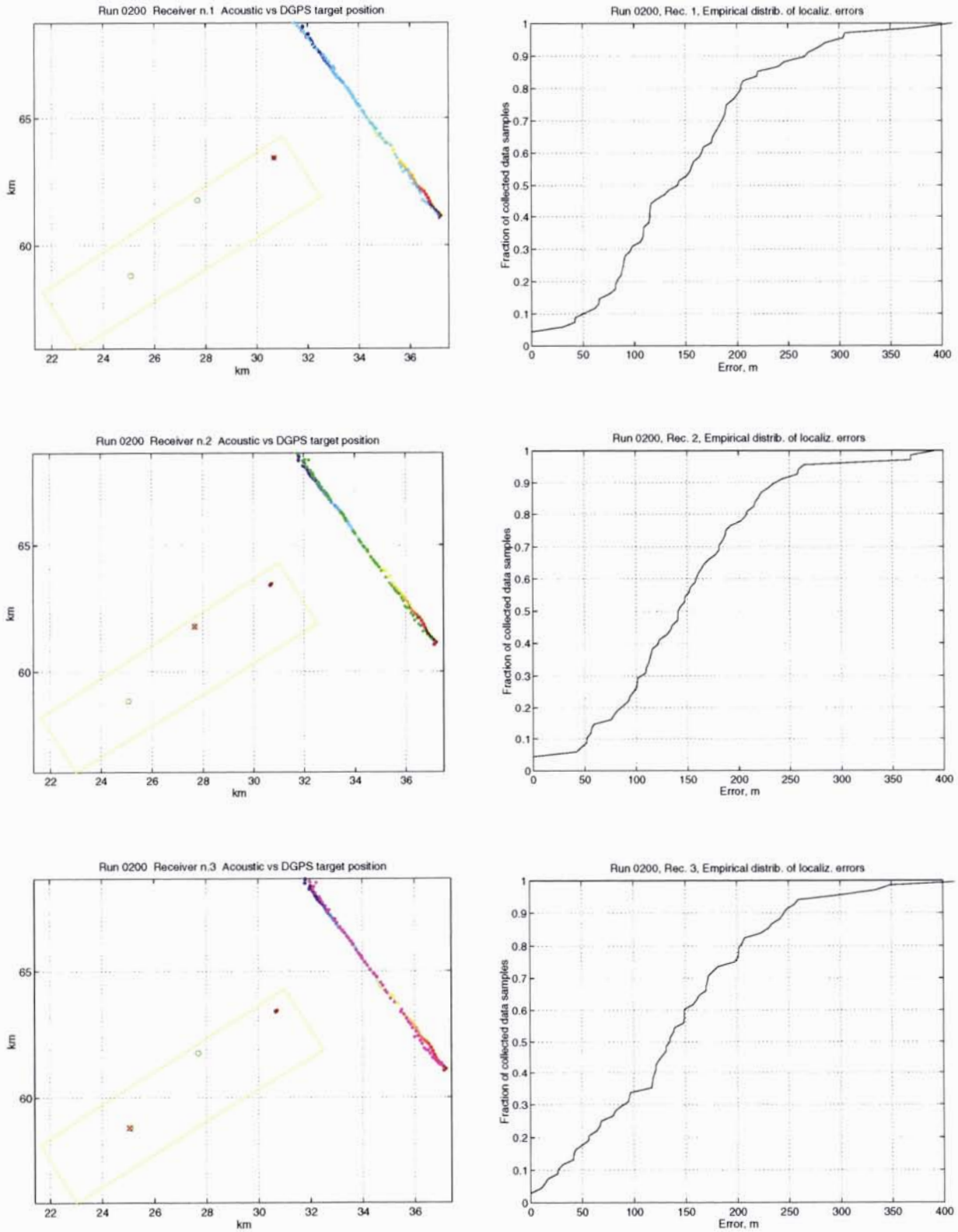

Figure B5. *Run 0200, 1.9 kHz, Trajectory D, Receiver 2.*

Annex C - Contact spreading data

Table C1 *Percentile and RMS values of contact spreading around the barycentre. (*): Receiver 1 not included.*

RUN	Frequency kHz	Target trajectory	Duration minutes	Contact Spreading $P_{0.5}$ m	Contact Spreading $P_{0.8}$ m	Contact Spreading RMS m
0103	3.5	C	90	60	111	110
0203	3.5	A	120	50	71	62
0104	3.5	D	60	60	109	95
0201	1.9	C	120	70	158	118
0200	1.9	D	60	62	117	105

Figure C1 lists the empirical distribution plots for the runs in Table C1.

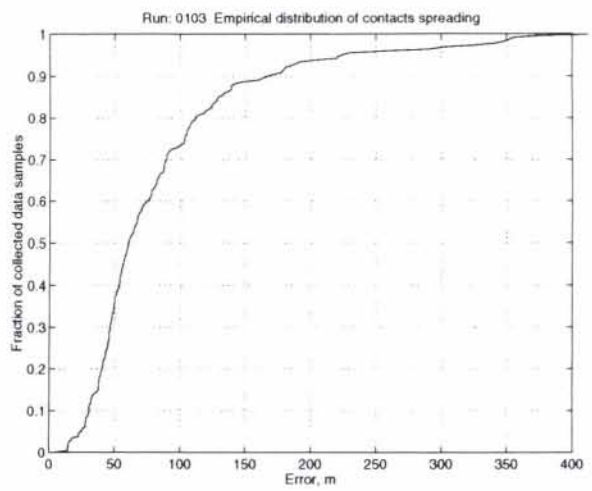

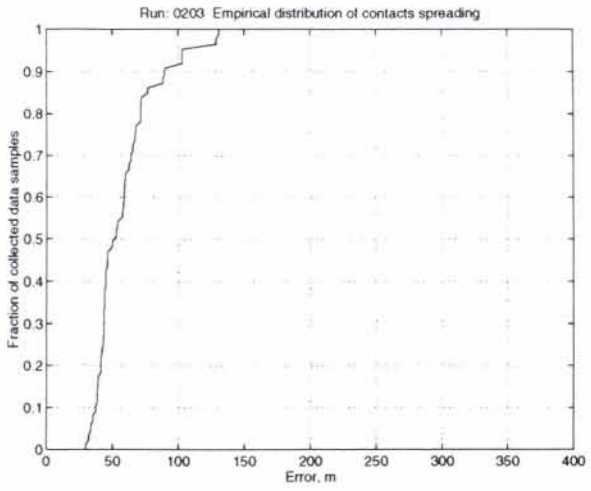

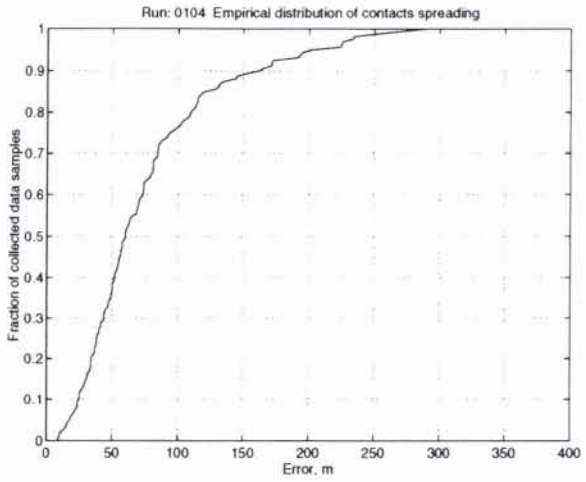

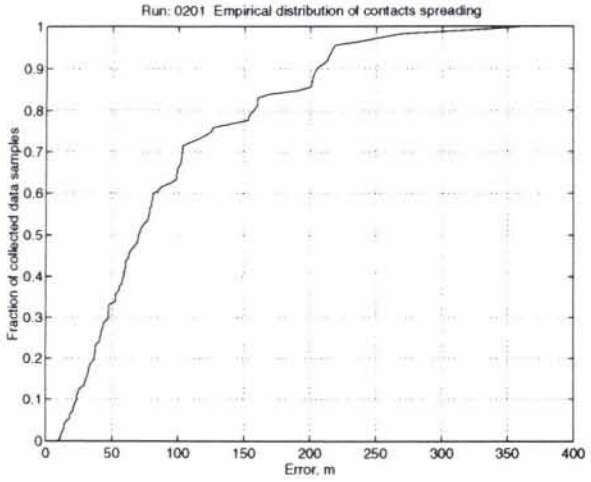

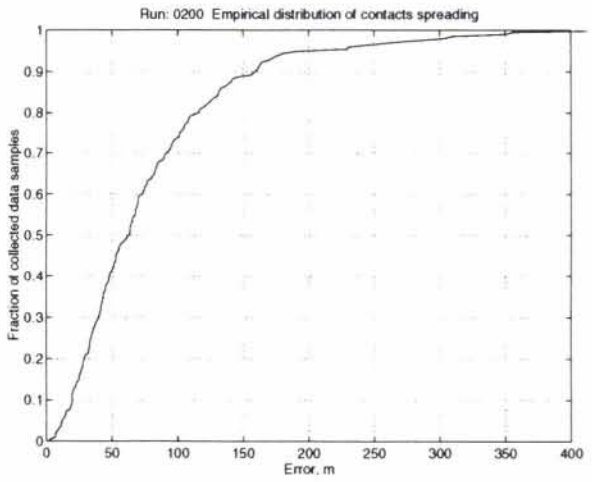

Figure C. *Empirical distributions of contacts spreading.*

Annex D - Contact fusion data

Figure D lists the empirical distribution plots described in Sect. 6.6 for all the runs.

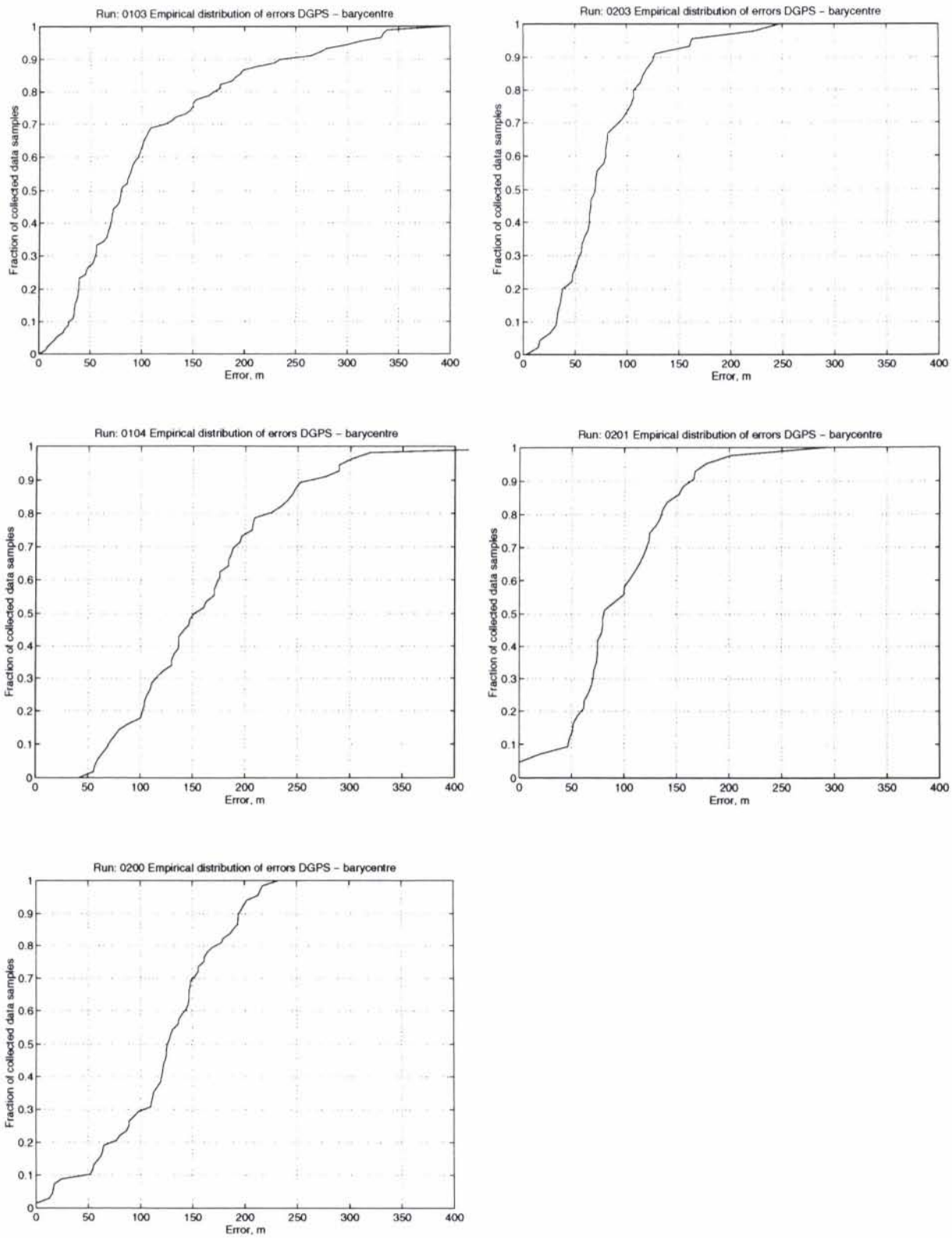

Figure D. *Empirical distributions of erros described in § 6.6.*

Report no. changed (Mar 2006): SR-291-UU

Document Data Sheet

Security Classification		Project No.
		021-1
Document Serial No.	**Date of Issue**	**Total Pages**
SR-291	December 1998	52 pp.

Author(s)

Mozzone, L., Bongi, S.

Title

Deployable Underwater Surveillance Systems. Localization and fusion of multistatic contacts. Evaluation of feasibility using experimental data.

Abstract

Deployable Underwater Surveillance Systems (DUSS) are a new active sonar concept based on a distributed network of small multistatic transmitter / receiver nodes. This study analyzes the contact localization capabilities of DUSS with both experimental data and simple modelling. Localization error medians of 118 m were measured analyzing 450 pings on 3 receivers in 2 frequencies and 3 target trajectories. This error produces a scattering of the contacts of the three receivers around their "barycentre", which is assumed by the multistatic system as the best estimation of the target position. Such scattering was found limited to an overall median value of 110 m. The integration of the distributed sonar nodes into a single, extended surveillance system is therefore possible with contact association windows of that size, corresponding to about 100 bearing - range cells. The resulting improvement of contact localization errors was estimated around 22 % with a very simple test. Efficient data fusion methods can therefore be investigated with good expectations. The experimental results do not depend on frequency, target range and trajectory, receiver monostatic / multistatic deployment geometry. Performance objectives and system specifications are also derived for prototype design. The precision of compasses and of assets deployment positioning is the most critical parameter, which needs improvements.

Keywords

Issuing Organization

North Atlantic Treaty Organization
SACLANT Undersea Research Centre
Viale San Bartolomeo 400, 19138 La Spezia, Italy

[From N. America: SACLANTCEN (New York) APO AE 09613]

Tel: +39 0187 527 361
Fax:+39 0187 524 600

E-mail: library@saclantc.nato.int

Initial Distribution for SR-291

Ministries of Defence

DND Canada	10
CHOD Denmark	8
MOD Germany	15
HNDGS Greece	12
MARISTAT Italy	9
MOD (Navy) Netherlands	12
NDRE Norway	10
MOD Portugal	5
MDN Spain	2
TDKK and DNHO Turkey	5
MOD UK	20
ONR USA	32

NATO Commands and Agencies

NAMILCOM	2
SACLANT	3
CINCEASTLANT/ COMNAVNORTHWEST	1
CINCIBERLANT	1
CINCWESTLANT	1
COMASWSTRIKFOR	1
COMSTRIKFLTANT	1
COMSUBACLANT	1
SACLANTREPEUR	1
SACEUR	2
CINCNORTHWEST	1
CINCSOUTH	1
COMEDCENT	1
COMMARAIRMED	1
COMNAVSOUTH	1
COMSTRIKFORSOUTH	1
COMSUBMED	1
NC3A	1
PAT	1

Scientific Committee of National Representatives

SCNR Belgium	1
SCNR Canada	1
SCNR Denmark	1
SCNR Germany	1
SCNR Greece	1
SCNR Italy	1
SCNR Netherlands	2
SCNR Norway	1
SCNR Portugal	1
SCNR Spain	1
SCNR Turkey	1
SCNR UK	1
SCNR USA	2
SECGEN Rep. SCNR	1
NAMILCOM Rep. SCNR	1

National Liaison Officers

NLO Canada	1
NLO Denmark	1
NLO Germany	1
NLO Italy	1
NLO Netherlands	1
NLO Spain	1
NLO UK	1
NLO USA	1

Sub-total	188
SACLANTCEN	30
Total	218